PAPER

Global well-posedness and Turing–Hopf bifurcation of prey-taxis systems with hunting cooperation

Weirun Tao[1] and Zhi-An Wang[2]

[1]School of Mathematics, Southeast University, Nanjing, China
[2]Department of Applied Mathematics, The Hong Kong Polytechnic University, Hong Kong, Hong Kong
Corresponding author: Zhi-An Wang; Email: mawza@polyu.edu.hk

Abstract

This paper is concerned with a predator–prey system with hunting cooperation and prey-taxis under homogeneous Neumann boundary conditions. We establish the existence of globally bounded solutions in two dimensions. In three or higher dimensions, the global boundedness of solutions is obtained for the small prey-tactic coefficient. By using hunting cooperation and prey species diffusion as bifurcation parameters, we conduct linear stability analysis and find that both hunting cooperation and prey species diffusion can drive the instability to induce Hopf, Turing and Turing–Hopf bifurcations in appropriate parameter regimes. It is also found that prey-taxis is a factor stabilizing the positive constant steady state. We use numerical simulations to illustrate various spatiotemporal patterns arising from the abovementioned bifurcations including spatially homogeneous and inhomogeneous time-periodic patterns, stationary spatial patterns and chaotic fluctuations.

1. Introduction

Prey-taxis, the movement of predators toward regions of higher prey density, plays important roles in biological control such as regulating prey (pest) population to avoid incipient outbreaks of prey or forming large-scale aggregation for survival (cf. [13, 32, 44]). This mechanism was first applied to the predator–prey systems by Kareiva and Odell [26] to interpret the heterogeneous aggregative patterns observed in a field experiment for one predator and one prey involving area-restricted search strategies. The Kareiva–Odell prey-taxis model generally reads as

$$\begin{cases} u_t = d_1 \Delta u - \chi \nabla \cdot (u \nabla v) + \beta G(v, u)u - \theta u, & x \in \Omega, \ t > 0, \\ v_t = d_2 \Delta v + F(v)v - G(v, u)u, & x \in \Omega, \ t > 0, \\ \frac{\partial u}{\partial \nu} = \frac{\partial v}{\partial \nu} = 0, & x \in \partial\Omega, \end{cases} \tag{1.1}$$

where $u(x, t)$ and $v(x, t)$ denote predator and prey density at position $x \in \Omega$ and time t, respectively, and $\Omega \subset \mathbb{R}^n (n \geq 1)$ is a bounded domain with smooth boundary. The function $G(v, u)$ is the functional response that describes the predator's consumption rate of prey, and $F(v)$ represents the per capita prey growth rate in the absence of predators. d_1 and d_2 are diffusion rates of the predator and the prey, respectively. The parameters β and θ represent the conversion rate of captured prey into predator and the predator mortality rate, respectively. All parameters are positive unless otherwise stated.

The functional response function $G(u, v)$ is a crucial factor shaping various dynamical behaviors in predator–prey systems [53]. Over the past century, different functional responses have been identified based on various biological applications, including Holling type [16–18], Hassell-Varley type [15], Beddington–DeAngelis type [4, 10], ratio-dependent type [3] and Crowley–Martin type [9], among

others [53]. The prey growth function $F(v)$ typically takes the form of a logistic type

$$F(v) = \sigma(1 - v/K) \tag{1.2}$$

with the prey intrinsic growth rate σ and the environmental carrying capacity K for the prey. Apart from the logistic type, $F(v)$ could be bistable (or Allee effect) type [55] or fear effect type [56], and so on. In the sequel, we shall assume $F(v)$ is of logistic type (1.2) unless otherwise stated.

This paper will be concerned with the functional response function employing the hunting cooperation strategy, which has attracted extensive attention recently. Cooperative hunting is a prominent behaviour among large social carnivores, which enhances their ability to capture prey in their natural habitats [34, 58]. This behaviour enables predators to subdue large prey and improve their hunting success. For instance, hyenas and wolves usually hunt alone when pursuing small-size prey such as gazelles and sheep. In contrast, they prefer to hunt in packs when hunting large-size prey such as zebras and deer [27, 33, 46]. This communal hunting phenomenon, leading to increased foraging efficiency, has been observed in higher predator densities of terrestrial carnivores, including lions [45], wolves [46] and African wild dogs [8]. To model this phenomenon of hunting cooperation, several functional responses that increase with respect to the predator density, also known as hunting cooperation functional responses, have been proposed, including

$$G(v, u) = \begin{cases} (\lambda + \alpha u)v, & \text{(Type I [51])}, \\ \dfrac{ce(\lambda + \alpha u)v}{1 + che(\lambda + \alpha u)v}, & \text{(Type II [5,7])}, \\ \dfrac{ce(\lambda + \alpha u)v^2}{1 + che(\lambda + \alpha u)v^2}, & \text{(Type III [53])}, \end{cases} \tag{1.3}$$

where $\lambda > 0$ represents the predation rate on prey and $\alpha \geq 0$ characterizes the level of predator cooperation during hunting, h represents the handling time per prey item, e_0 is the encounter rate per predator per prey unit time, and c is a fraction of a prey item killed per predator per encounter. When $\alpha = 0$, the Type I, II and III hunting cooperation response functions reduce to the well-known Holling I, II and III functional response functions, respectively.

Among other things, this paper is focused on the Type I hunting cooperation:

$$G(v, u) = (\lambda + \alpha u)v \tag{1.4}$$

which was first proposed in [52] and the corresponding temporal system (namely system (1.1) with (1.4) and $d_1 = d_2 = \chi = 0$) was numerically studied in [52]. It was found that hunting cooperation can benefit predator populations by increasing attack rates, and large values of α can induce Hopf bifurcations.

The system (1.1) with $\chi = 0$ is referred to as the diffusive predator–prey system. It was shown that (1.1) with (1.4) will not have Turing instability without hunting cooperation (i.e. $\alpha = 0$) (cf. [6, 60]), while it will do with hunting cooperation (i.e. $\alpha > 0$) only if the predator spreads slower than the prey (i.e. $d_1 > d_2$) (cf. [6, 47, 60]). Later, the Hopf bifurcation was investigated in [29] by the centre manifold and the normal form theory. If the Neumann boundary condition was replaced by the homogeneous Dirichlet boundary condition $u|_{\partial\Omega} = v|_{\partial\Omega} = 0$ and $n < 6$, the stationary solution of the system (1.1) with (1.4) was studied in [40] showing that sufficiently large α leads to the extinction of the predator species. For more related works on the predator–prey models with hunting cooperation, we refer readers to [14, 20, 28, 50, 54] for Allee effects in prey, [35] for fear effects in prey, [12] for group defense in prey, [48] for three-species food chain, [11, 31, 41, 51, 54] for hunting cooperation functional response functions other than Type I, and references therein.

Though a considerable body of literature has studied the dynamics of predator–prey systems with hunting cooperation in the absence of prey-taxis (i.e. $\chi = 0$) as mentioned above, only a few results are available to the predator–prey systems with prey-taxis and hunting cooperation (cf. [38, 42, 43, 62]). When the hunting cooperation functional response function $G(u, v)$ is Type II as given in (1.3), the existence of non-constant positive steady states of prey-taxis system (1.1) was obtained by the bifurcation theory in one dimension in [37] where it was also shown that small prey-tactic sensitivity $\chi > 0$ can

induce the Turing instability. Recently the work [62] established the existence of globally bounded classical solutions of (1.1) with Type II hunting cooperation in any dimension, and showed that negative prey-tactic sensitivity $\chi < 0$ (i.e. repulsive prey-taxis) can induce the Turing instability. When the hunting cooperation functional response function $G(u, v)$ is uniformly bounded for all $u, v \geq 0$, the global boundedness of solutions was established [42, 43] where the global stability of constant positive steady states and existence/nonexistence of non-constant positive solutions were further obtained if $G(u, v)$ is Type II. We remak the assumption in [42, 43] rules out the Type I hunting cooperation functional response function (1.4) since it is obviously not uniformly bounded for $u, v \geq 0$.

It is seen from the abovementioned existing results that the prey-taxis system (1.1) with Type I hunting cooperation functional response function $G(u, v)$ has not been studied, which is the most difficult case to study from a mathematical point of view among three types given in (1.3) since $G(u, v)$ is not uniformly bounded for $u, v \geq 0$ if it is of Type I. When $G(u, v)$ is uniformly bounded for all $u, v \geq 0$ like Type II or Type III, the regularity of the Neumann heat semigroup (cf. [36]) can be directly applied to establish global boundedness of solutions, while Type I forfeits this advantage. Apart from this, it is also unclear whether the Type I hunting cooperation may induce the spatiotemporal patterns. This paper will address these questions and we therefore consider the following prey-taxis system (1.1) with Type I hunting cooperation

$$
\begin{cases}
u_t = d_1 \Delta u - \chi \nabla \cdot (u \nabla v) + u \left[\beta \left(\lambda + \alpha u \right) v - \theta \right], & x \in \Omega, \ t > 0, \\
v_t = d_2 \Delta v + \sigma v \left(1 - \frac{v}{K} \right) - \left(\lambda + \alpha u \right) uv, & x \in \Omega, \ t > 0, \\
\frac{\partial u}{\partial v} = \frac{\partial v}{\partial v} = 0, & x \in \partial \Omega, \\
u(x, 0) = u_0(x), \ v(x, 0) = v_0(x), & x \in \Omega,
\end{cases}
\tag{1.5}
$$

where the parameters $d_1, d_2, \beta, \lambda, \alpha, \theta, \sigma, K > 0$ and $\chi \geq 0$ have the same biological interpretations as mentioned above. To reduce the number of parameters, we introduce the following rescalings

$$
\tilde{d}_1 = \frac{d_1}{\theta}, \quad \tilde{d}_2 = \frac{d_2}{\theta}, \quad \tilde{\chi} = \frac{\chi}{\beta \lambda}, \quad \tilde{\sigma} = \frac{\sigma}{\theta}, \quad \tilde{K} = \frac{\beta \lambda K}{\theta}, \quad \tilde{\alpha} = \frac{\alpha \theta}{\lambda^2},
$$

and

$$
\tilde{u} = \frac{\lambda u}{\theta}, \quad \tilde{v} = \frac{\beta \lambda v}{\theta}, \quad \tilde{t} = \theta t.
$$

Substituting the above rescalings into (1.5) and dropping the tildes for brevity, we obtain the following rescaled system

$$
\begin{cases}
u_t = d_1 \Delta u - \chi \nabla \cdot (u \nabla v) + (1 + \alpha u) uv - u, & x \in \Omega, \ t > 0, \\
v_t = d_2 \Delta v + \sigma v \left(1 - \frac{v}{K} \right) - (1 + \alpha u) uv, & x \in \Omega, \ t > 0, \\
\frac{\partial u}{\partial v} = \frac{\partial v}{\partial v} = 0, & x \in \partial \Omega, \\
u(x, 0) = u_0(x), \ v(x, 0) = v_0(x), & x \in \Omega,
\end{cases}
\tag{1.6}
$$

where the parameters $d_1, d_2, \alpha, K, \sigma$ are positive and $\chi > 0$. Throughout the paper, we shall often use the following notations

$$
f(u, v) := (1 + \alpha u) uv - u \quad \text{and} \quad g(u, v) := \sigma v \left(1 - \frac{v}{K} \right) - (1 + \alpha u) uv
\tag{1.7}
$$

for brevity.

The main analytical result of this paper is the following.

Theorem 1.1. *Let $\Omega \subset \mathbb{R}^n$ ($n \geq 2$) be a bounded domain with smooth boundary, and let $(u_0, v_0) \in [W^{1,q}(\Omega)]^2$ with some $q > n$ and $u_0(x), v_0(x) \geq 0 (\not\equiv 0)$. Then there exists $\chi_* \in (0, +\infty]$ such that for all $\chi \in (0, \chi_*)$, the system (1.6) admits a unique classical solution $(u, v) \in [C^0(\overline{\Omega} \times [0, \infty)) \cap C^{2,1}(\overline{\Omega} \times (0, \infty))]^2$ satisfying $u, v > 0$ for all $t > 0$. Moreover, there exists a constant $C > 0$ independent of t such that*

$$
\|u(\cdot, t)\|_{L^\infty(\Omega)} + \|v(\cdot, t)\|_{L^\infty(\Omega)} \leq C \quad \text{for all } t > 0.
$$

In particular, $\chi_* = +\infty$ if $n = 2$.

Before ending this section, we outline the main difficulties and proof strategies.

1.1 Sketch of proof strategies

Without prey-taxis (i.e. $\chi = 0$), problem (1.6) can be regarded as a special one considered in [38]. Then the global boundedness of solutions to (1.6) with $\chi = 0$ in any dimension ($n \geq 1$) is a consequence of [38, Theorem 3.1] (see also [19]) based on the L^p-duality method. Without hunting cooperation (i.e. $\alpha = 0$), the global boundedness of solutions to (1.6) has been established in [23, 61]. Now with $\alpha > 0$, the source term contains a cubic polynomial $\alpha u^2 v$ and many arguments and estimates in [23, 61] for the quadratic polynomial are no longer applicable. Hence, new technical ingredients are needed to deal with the higher-order nonlinearity. Below we briefly describe our strategies used to obtain the global boundedness of solutions for $n = 2$ and $n \geq 3$.

(i) $n = 2$. In this case, by fully exploiting the model structural feature, we use cancellation ideas to handle the troubling prey-taxis term while simultaneously controlling the cubic nonlinear source term $\alpha u^2 v$ (see the proof of Lemma 3.1), and finally obtain the crucial uniform-in-time bound of $\|u\|_{L^2(\Omega)}$ with sophisticated coupling estimates by establishing a Grownwall type inequality for the linear combination of following four terms (see (3.19) and (3.27))

$$\frac{d}{dt}\int_\Omega u^2, \quad \frac{d}{dt}\int_\Omega \frac{|\nabla v|^2}{v}, \quad \frac{d}{dt}\int_\Omega u\ln u, \quad \frac{d}{dt}\int_\Omega uv.$$

Then we further perform L^p estimates to obtain the uniform-in-time bound of $\|u\|_{L^p(\Omega)}$ for $p > 2$, which yields the global boundedness of solutions by the boundedness criterion in Lemma 2.6 and the extension criterion in Lemma 2.1. We stress that here we obtain the L^2-estimates directly with the sophisticated coupling estimates by fully exploiting the advantage of cubic decay term $-\alpha u^2 v$. This is different from the estimates in the existing literature for the prey-taxis model without hunting cooperation such as [23, 61] where the L^2-estimate of u is established based on the estimate of $\|u\ln u\|_{L^1}$ and $\|\nabla v\|_{L^2}$ which are first obtained separately.

(ii) $n \geq 3$. In this case, we first establish a uniform-in-time bound of the weighted L^p-norm $\int_\Omega u^p\varphi(v)$ ($p > 1$) by constructing an appropriate weight function $\varphi(v)$ (see Lemma 4.1 and Lemma 4.2), and then obtain a bound of $\|u\|_{L^p(\Omega)}$ under a smallness condition on $\chi > 0$.

The rest of the paper is organized as follows. In Sect. 2, we establish the local existence of solutions to the system (1.6) and derive some preliminary results. We prove Theorem 1.1 for $n = 2$ in Sect. 3 and for $n \geq 3$ in Sect. 4. Finally, in Sect. 5, we conduct linear stability analysis to show that both Turing bifurcations and Turing–Hopf bifurcations may arise from the system (1.6), and use numerical simulations to demonstrate that (1.6) may generate various complex spatiotemporal patterns such as spatially homogeneous time-periodic patterns, stationary patterns, spatiotemporal periodic patterns and chaos.

2. Local existence and preliminaries

In this section, we establish the local existence of solutions to the system (1.6) and provide some preliminary results. Hereafter, we use C and C_i ($i = 1, 2, 3, \cdots$) to denote generic positive constants that may vary from line to line in the context. We begin with the local existence of solutions.

Lemma 2.1. *Suppose that the assumptions in Theorem 1.1 hold. Then there exists $T_{\max} \in (0, +\infty]$ such that the system (1.6) has a unique classical solution*

$$(u, v) \in \left[C^0(\overline{\Omega} \times (0, T_{\max})) \cap C^{2,1}(\overline{\Omega} \times (0, T_{\max})) \right]^2$$

satisfying

$$u > 0 \quad and \quad 0 < v \leq M_0 := \max\left\{\|v_0\|_{L^\infty(\Omega)}, K\right\} \quad for\ all\ (x, t) \in \Omega \times (0, T_{\max}). \tag{2.1}$$

Moreover,

$$either \quad T_{\max} = +\infty \quad or \quad \limsup_{t \nearrow T_{\max}} \left(\|u(\cdot, t)\|_{L^\infty(\Omega)} + \|v(\cdot, t)\|_{L^\infty(\Omega)}\right) = +\infty. \tag{2.2}$$

Proof. Denote $\omega = (u, v)$. Then the system (1.6) can be written as

$$\begin{cases} \omega_t = \nabla \cdot (\mathbb{A}(\omega)\nabla\omega) + \Phi(\omega), & x \in \Omega, t > 0, \\ \frac{\partial\omega}{\partial\nu} = 0, & x \in \partial\Omega, \\ \omega(x, 0) = (u_0(x), v_0(x)), & x \in \Omega, \end{cases}$$

where $\mathbb{A}(\omega) = \begin{bmatrix} d_1 & -\chi u \\ 0 & d_2 \end{bmatrix}$ and $\Phi(\omega) = \begin{pmatrix} f(u, v) \\ g(u, v) \end{pmatrix}$ with $f(u, v)$ and $g(u, v)$ given by (1.7). The upper triangular matrix $\mathbb{A}(\omega)$ is positively definite. Hence, the system (1.6) is normally parabolic. Then the local existence and uniqueness of classical solutions follow from Amann's theorem [1, Theorem 7.3 and Corollary 9.3] and the blow-up criteria (2.2) follows from [2, Theorem 15.5]. Moreover, $u, v > 0$ for $(x, t) \in \Omega \times (0, T_{\max})$ can be established by the strong maximum principle along with $u_0, v_0 \geq 0 (\not\equiv 0)$. These arguments are standard and we refer readers to [57, Lemma 2.6] and [24, Lemma 2.1] for details. Finally, an application of [23, Lemma 2.2] proves $v \leq M_0$ for $(x, t) \in \Omega \times (0, T_{\max})$. □

The following result can be easily obtained.

Lemma 2.2. *Suppose that the assumptions in Theorem 1.1 hold and (u, v) is the solution of the system (1.6). Then*

$$\|u(\cdot, t)\|_{L^1(\Omega)} \leq M_1 := \max\left\{\|u_0 + v_0\|_{L^1(\Omega)}, \frac{K(1+\sigma)^2}{4\sigma}|\Omega|\right\} \quad for\ all\ t \in (0, T_{\max}). \tag{2.3}$$

Proof. Adding the first two equations of (1.6), integrating the resulting equation by parts and using Young's inequality $(1+\sigma)v \leq \frac{\sigma}{K}v^2 + \frac{K(1+\sigma)^2}{4\sigma}$, we have

$$\frac{d}{dt}\int_\Omega (u + v) = \sigma\int_\Omega v\left(1 - \frac{v}{K}\right) - \int_\Omega u \leq -\int_\Omega (u + v) + \frac{K(1+\sigma)^2}{4\sigma}|\Omega| \quad for\ all\ t \in (0, T_{\max}),$$

which alongside $u, v \geq 0$ implies

$$\int_\Omega (u + v) \leq \max\left\{\|u_0 + v_0\|_{L^1(\Omega)}, \frac{K(1+\sigma)^2}{4\sigma}|\Omega|\right\}.$$

The proof is completed. □

We shall recall some inequalities that will be used later.

Lemma 2.3 ([22, Lemma 2.3]). *Let $\alpha, \beta, T > 0$, $\tau \in (0, T)$, and suppose that $\phi:[0, T) \to [0, \infty)$ is absolutely continuous satisfying*

$$\phi'(t) + \phi^{1+\sigma}(t) \leq \varphi(t)\phi(t) + h(t), \quad t > 0,$$

where $\sigma > 0$ is a constant, $\varphi(t), h(t) \geq 0$ with $\varphi(t), h(t) \in L^1_{loc}([0, T))$ and

$$\sup_{t \in [\tau, T)}\int_{t-\tau}^t \varphi(s)ds \leq \alpha, \quad \sup_{t \in [\tau, T)}\int_{t-\tau}^t h(s)ds \leq \beta.$$

Then for any $t > t_0$, we have

$$\phi(t) \leq \phi(t_0)\, e^{\int_{t_0}^t \varphi(s)ds} + \int_{t_0}^t h(\tau)e^{\int_\tau^t \varphi(s)ds}d\tau \tag{2.4}$$

and

$$\sup_{t \in (0,T)} \phi(t) \le \sigma \left(\frac{2A}{1+\sigma} \right)^{\frac{1+\sigma}{\sigma}} + 2B, \quad \sup_{t \in [\tau,T)} \int_{t-\tau}^{t} \phi^{1+\sigma}(s)ds \le (1+\alpha) \sup_{t \in (0,T)} \{\phi(t)\} + \beta, \tag{2.5}$$

where

$$A = \tau^{-\frac{1}{1+\sigma}} (1+\alpha)^{\frac{1}{1+\sigma}} e^{2\alpha}, \quad B = \tau^{-\frac{1}{1+\sigma}} \beta^{\frac{1}{1+\sigma}} e^{2\alpha} + 2\beta e^{2\alpha} + \phi(0)e^{\alpha}. \tag{2.6}$$

Lemma 2.4 ([59, Lemma 3.3]). *Suppose that $H \in C^1((0,\infty), \mathbb{R}_+)$ and $\Theta(s) := \int_1^s \frac{d\sigma}{H(\sigma)}$ for $s > 0$. Then for all $\varphi \in C^2(\overline{\Omega})$ fulfilling $\frac{\partial \varphi}{\partial \nu} = 0$ on $\partial\Omega$, it holds that*

$$\int_\Omega \frac{H'(\varphi)}{H^3(\varphi)} |\nabla\varphi|^4 \le (2+\sqrt{n})^2 \int_\Omega \frac{H(\varphi)}{H'(\varphi)} \left| D^2\Theta(\varphi) \right|^2.$$

Lemma 2.5 ([30, Lemma 4.2]). *Assume that Ω is a bounded domain, and let $w \in C^2(\overline{\Omega})$ satisfy $\frac{\partial w}{\partial \nu} = 0$ on $\partial\Omega$. Then we have*

$$\frac{\partial |\nabla w|^2}{\partial \nu} \le 2\kappa |\nabla w|^2,$$

where $\kappa = \kappa(\Omega)$ is an upper bound of the curvatures of $\partial\Omega$.

Now we establish a boundedness criterion.

Lemma 2.6. *Suppose that the assumptions in Theorem 1.1 hold and (u,v) is the solution of the system (1.6). If there exists $p > \frac{3n}{2}$ ($n \ge 2$) such that*

$$\sup_{t \in (0,T_{\max})} \|u(\cdot,t)\|_{L^p(\Omega)} \le K_1 \tag{2.7}$$

for a positive constant K_1, there exists a positive constant K_2 independent of t such that

$$\|u(\cdot,t)\|_{L^\infty(\Omega)} \le K_2 \quad \text{for all } t \in (0, T_{\max}).$$

Proof. Assume that (2.7) holds for some $p > \frac{3n}{2}$ ($n \ge 2$). Then there exists a constant $C_1 > 0$ such that

$$\sup_{t \in (0,T_{\max})} \|u^2(\cdot,t)\|_{L^{\frac{p}{2}}(\Omega)} \le C_1.$$

Since $\frac{p}{2} > \frac{3n}{4}$, one can use a standard argument based on the smooth property of the Neumann heat semigroup (cf. [36]) to find two constants $r_1 > 3n$ and $C_2 > 0$ such that

$$\sup_{t \in (0,T_{\max})} \|\nabla v(\cdot,t)\|_{L^{r_1}(\Omega)} \le C_2. \tag{2.8}$$

Given $t \in (0, T_{\max})$, we let $t_0 := (t-1)_+$. By Duhamel's principle, u can be represented as

$$u(\cdot,t) = e^{d_1(t-t_0)\Delta} u(\cdot, t_0) - \chi \int_{t_0}^t e^{d_1(t-s)\Delta} \nabla \cdot [u(\cdot,s)\nabla v(\cdot,s)] \, ds + \int_{t_0}^t e^{d_1(t-s)\Delta} f(u(\cdot,s), v(\cdot,s)) ds$$

$$=: I_1 + I_2 + I_3 \quad \text{for all } t \in (0, T_{\max}). \tag{2.9}$$

By (2.3), the maximum principle and the smooth property of the Neumann heat semigroup again, for all $t \in (0, T_{\max})$, we can find two positive constants C_3 and C_4 such that

$$\|I_1\|_{L^\infty(\Omega)} = \begin{cases} \|e^{d_1 t\Delta} u(\cdot,0)\|_{L^\infty(\Omega)} \le \|u_0\|_{L^\infty(\Omega)}, & \text{if } t \le 1, \\ \|e^{d_1\Delta} u(\cdot,t-1)\|_{L^\infty(\Omega)} \le C_3 \|u(\cdot,t-1)\|_{L^1(\Omega)} \le C_4, & \text{if } t > 1. \end{cases} \tag{2.10}$$

Let $r_2 := \frac{pr_1}{p+r_1}$. Then $r_2 > n$ due to $\frac{1}{r_2} = \frac{1}{p} + \frac{1}{r_1} < \frac{1}{n}$. By (2.8) and Hölder's inequality, for all $t \in (0, T_{\max})$, we have

$$\sup_{t \in (0,T_{\max})} \|u(\cdot,t)\nabla v(\cdot,t)\|_{L^{r_2}(\Omega)} \le \sup_{t \in (0,T_{\max})} \|u(\cdot,t)\|_{L^p(\Omega)} \|\nabla v(\cdot,t)\|_{L^{r_1}(\Omega)} \le K_1 C_2,$$

which alongside the smooth property of the Neumann heat semigroup gives two positive constants C_5 and C_6 such that

$$\|I_2\|_{L^\infty(\Omega)} \le C_5 \int_{t_0}^t \left(1 + (t-s)^{-\frac{1}{2}-\frac{n}{2r_2}}\right) e^{-\lambda_1 d_1(t-s)} \|u(\cdot,s)\nabla v(\cdot,s)\|_{L^{r_2}(\Omega)} ds \le C_6 \tag{2.11}$$

for all $t \in (0, T_{\max})$, where we have used the fact $\frac{1}{2} + \frac{n}{2r_2} < 1$, and $\lambda_1 > 0$ denotes the first nonzero eigenvalue of $-\Delta$ in Ω under the homogeneous Neumann boundary condition.

It follows from (1.7), (2.1), (2.7), Young's inequality and Hölder's inequality that there exist two constants $C_7, C_8 > 0$ such that

$$\int_\Omega |f(u(\cdot,t), v(\cdot,t))|^{\frac{3n}{4}} \le C_7 \int_\Omega \left(u^{\frac{3n}{2}} + 1\right) \le C_8 \quad \text{for all } t \in (0, T_{\max}). \tag{2.12}$$

Let $\bar{f}(t) := \frac{1}{|\Omega|} \int_\Omega f(u(\cdot,t), v(\cdot,t))$ for all $t \in (0, T_{\max})$. Notice that $\frac{3n}{4} > 1$ for $n \ge 2$. Then (2.12) and Hölder's inequality imply

$$|\bar{f}(t)| \le \frac{1}{|\Omega|} \int_\Omega (|f(u(\cdot,t), v(\cdot,t))|^{\frac{3n}{4}} + 1) \le \frac{C_8}{|\Omega|} + 1 \quad \text{for all } t \in (0, T_{\max}). \tag{2.13}$$

Using (2.12), (2.13), $t - t_0 \le 1$, and the L^p-L^q estimates of the Neumann heat semigroup, we can find two positive constants C_9 and C_{10} satisfying

$$
\begin{aligned}
\|I_3\|_{L^\infty(\Omega)} &\le \int_{t_0}^t \|e^{d_1(t-s)\Delta} f(\cdot,s)\|_{L^\infty(\Omega)} ds \\
&\le \int_{t_0}^t \|e^{d_1(t-s)\Delta}(f(\cdot,s) - \bar{f}(s))\|_{L^\infty(\Omega)} ds + \int_{t_0}^t \|e^{d_1(t-s)\Delta} \bar{f}(s)\|_{L^\infty(\Omega)} ds \\
&\le C_9 \int_{t_0}^t (1 + (t-s)^{-\frac{2}{3}}) e^{-\lambda_1 d_1(t-s)} \|f(\cdot,s) - \bar{f}(s)\|_{L^{\frac{3n}{4}}(\Omega)} ds + \int_{t_0}^t \left(\frac{C_8}{|\Omega|} + 1\right) ds \\
&\le C_{10} \quad \text{for all } t \in (0, T_{\max}).
\end{aligned}
\tag{2.14}
$$

The combination of (2.9), (2.10), (2.11) and (2.14) yields that

$$\sup_{t \in (0, T_{\max})} \|u(\cdot,t)\|_{L^\infty(\Omega)} \le C_{11} \quad \text{for all } t \in (0, T_{\max})$$

with a constant $C_{11} > 0$. The proof is completed. $\qquad\square$

3. Proof of Theorem 1.1 for $n = 2$

This section is devoted to proving Theorem 1.1 for $n = 2$. To this end, we construct an appropriate functional in the form of a linear combination of the four terms

$$\frac{d}{dt}\int_\Omega \frac{|\nabla v|^2}{v}, \quad \frac{d}{dt}\int_\Omega u \ln u, \quad \frac{d}{dt}\int_\Omega u^2, \quad \frac{d}{dt}\int_\Omega uv$$

to derive some *a priori* estimates including the time-independent boundedness of $\|u\|_{L^2(\Omega)}$. This idea was first used in [59] for a chemotaxis-fluid model, and then developed for predator–prey models with prey-taxis [23, 25].

3.1 L^2-estimate via sophisticated coupling estimates

Lemma 3.1 *Suppose that the assumptions in Theorem 1.1 hold with $n = 2$ and (u, v) is the solution of the system (1.6). Then for $\tau \in (0, T_{\max})$, we have*

$$\int_\Omega \frac{|\nabla v|^2}{v} + \int_\Omega u^2 \le C \quad \text{for all } t \in (0, T_{\max}) \tag{3.1}$$

and

$$\int_t^{t+\tau} \int_\Omega \left(\frac{|D^2 v|^2}{v} + \frac{|\nabla v|^4}{v^3} + \frac{|\nabla u|^2}{u} + |\nabla u|^2 + u^2 |\nabla v|^2 \right) (\cdot, s) ds \le C(\tau + 1) \tag{3.2}$$

for all $t \in (0, T_{\max} - \tau)$, *where* $D^2 v$ *denotes the Hessian matrix of v.*

Proof. We split the proof into several steps.

Step 1. An inequality for $\frac{d}{dt} \int_\Omega \frac{|\nabla v|^2}{v}$. For all $t \in (0, T_{\max})$, it holds that

$$\begin{aligned}
\frac{1}{2} \frac{d}{dt} \int_\Omega \frac{|\nabla v|^2}{v} &= -\frac{1}{2} \int_\Omega \frac{|\nabla v|^2}{v^2} v_t + \int_\Omega \frac{\nabla v \cdot \nabla v_t}{v} \\
&= \frac{1}{2} \int_\Omega \frac{|\nabla v|^2}{v^2} v_t - \int_\Omega \frac{\Delta v}{v} v_t \\
&= \underbrace{d_2 \left(\frac{1}{2} \int_\Omega \frac{|\nabla v|^2}{v^2} \Delta v - \int_\Omega \frac{|\Delta v|^2}{v} \right)}_{= I_4} + \frac{1}{2} \int_\Omega \frac{|\nabla v|^2}{v^2} g(u, v) - \int_\Omega \frac{\Delta v}{v} g(u, v).
\end{aligned} \tag{3.3}$$

We have from (1.7) and (2.1) that

$$\frac{1}{2} \int_\Omega \frac{|\nabla v|^2}{v^2} g(u, v) \le \frac{1}{2} \int_\Omega \frac{|\nabla v|^2}{v^2} \left(\sigma v - \alpha u^2 v \right) \le \frac{\sigma}{2} \int_\Omega \frac{|\nabla v|^2}{v} - \frac{\alpha}{2M_0} \int_\Omega u^2 |\nabla v|^2 \tag{3.4}$$

for all $t \in (0, T_{\max})$. For the term I_4, we claim that there exists a positive constant C_1 such that

$$I_4 \le -\frac{3A_1}{4} \int_\Omega \left(\frac{|D^2 v|^2}{v} + \frac{|\nabla v|^4}{v^3} \right) + C_1 \int_\Omega \frac{|\nabla v|^2}{v} \quad \text{for all } t \in (0, T_{\max}), \tag{3.5}$$

where $A_1 = \frac{d_2}{3(2+\sqrt{2})^2 + 2}$. Then the combination of (3.3)-(3.5) indicates that

$$\begin{aligned}
&\frac{1}{2} \frac{d}{dt} \int_\Omega \frac{|\nabla v|^2}{v} + \frac{1}{2} \int_\Omega \frac{|\nabla v|^2}{v} + \frac{3A_1}{4} \int_\Omega \left(\frac{|D^2 v|^2}{v} + \frac{|\nabla v|^4}{v^3} \right) \\
&\le -\frac{\alpha}{2M_0} \int_\Omega u^2 |\nabla v|^2 + \left(\frac{1+\sigma}{2} + C_1 \right) \int_\Omega \frac{|\nabla v|^2}{v} - \int_\Omega \frac{\Delta v}{v} g(u, v) \quad \text{for all } t \in (0, T_{\max}).
\end{aligned} \tag{3.6}$$

Using (2.1) and Young's inequality, we obtain

$$\left(\frac{1+\sigma}{2} + C_1 \right) \int_\Omega \frac{|\nabla v|^2}{v} \le \frac{A_1}{4} \int_\Omega \frac{|\nabla v|^4}{v^3} + \frac{\left(\frac{1+\sigma}{2} + C_1 \right)^2}{A_1} \int_\Omega v \le \frac{A_1}{4} \int_\Omega \frac{|\nabla v|^4}{v^3} + C_2 \tag{3.7}$$

for all $t \in (0, T_{\max})$, where $C_2 := \frac{M_0 |\Omega|}{A_1} \left(\frac{1+\sigma}{2} + C_1 \right)^2$. By (1.7), we have

$$-\int_\Omega \frac{\Delta v}{v} g(u, v) = -\int_\Omega \Delta v \left(\sigma \left(1 - \frac{v}{K} \right) - (1 + \alpha u) u \right) = -\frac{\sigma}{K} \int_\Omega |\nabla v|^2 - I_5 \le -I_5, \tag{3.8}$$

where $I_5 := \int_\Omega (1 + 2\alpha u) \nabla u \cdot \nabla v$. Substituting (3.7) and (3.8) into (3.6), we have

$$\frac{1}{2} \frac{d}{dt} \int_\Omega \frac{|\nabla v|^2}{v} + \frac{1}{2} \int_\Omega \frac{|\nabla v|^2}{v} + \frac{A_1}{2} \int_\Omega \left(\frac{|D^2 v|^2}{v} + \frac{|\nabla v|^4}{v^3} \right) \le C_2 - \frac{\alpha}{2M_0} \int_\Omega u^2 |\nabla v|^2 - I_5 \tag{3.9}$$

for all $t \in (0, T_{\max})$.

We next prove (3.5) by similar arguments to that of [23, 3.2 and Lemma 3.3] (see also the proof of [25, 3.2 and Lemma 3.3]). For completeness, we sketch the proof here. Applying [23, Eqs. (3.19) and (3.27)] with $F(v) = v$ therein, we have

$$I_4 = \frac{d_2}{2} \int_{\partial \Omega} \frac{1}{v} \cdot \frac{\partial |\nabla v|^2}{\partial \nu} - d_2 \int_\Omega v |D^2 \ln v|^2 \quad \text{for all } t \in (0, T_{\max}) \tag{3.10}$$

and

$$\int_\Omega \frac{|D^2 v|^2}{v} \le 2 \left((2+\sqrt{2})^2 + 1 \right) \int_\Omega v |D^2 \ln v|^2 \quad \text{for all } t \in (0, T_{\max}). \tag{3.11}$$

Using Lemma 2.4 with $H(v) = v$ yields

$$\int_\Omega \frac{|\nabla v|^4}{v^3} \le (2+\sqrt{2})^2 \int_\Omega v |D^2 \ln v|^2 \quad \text{for all } t \in (0, T_{\max}). \tag{3.12}$$

To proceed, we recall the trace inequality [39, Remark 52.9]: for any $\varepsilon > 0$, there exists a constant $C(\varepsilon) > 0$ such that

$$\|w\|_{L^2(\partial\Omega)} \le \varepsilon \|\nabla w\|_{L^2(\Omega)} + C(\varepsilon) \|w\|_{L^2(\Omega)} \quad \text{for } w \in W^{1,2}(\Omega). \tag{3.13}$$

Denote $\varphi_0(v) = \frac{|\nabla v|}{\sqrt{v}}$. Then for all $t \in (0, T_{\max})$, it follows from Young's inequality that

$$|\nabla \varphi_0(v)|^2 = \left(\frac{D^2 v \cdot \nabla v}{\sqrt{v} |\nabla v|} - \frac{|\nabla v| \nabla v}{2 v^{\frac{3}{2}}} \right)^2 \le \frac{|D^2 v|^2}{v} + \frac{|D^2 v| \cdot |\nabla v|^2}{v^2} + \frac{|\nabla v|^4}{4 v^3} \le \frac{5}{4} \left(\frac{|D^2 v|^2}{v} + \frac{|\nabla v|^4}{v^3} \right).$$

This alongside Lemma 2.5, (3.13) with $\varepsilon = \sqrt{\frac{A_1}{10\kappa d_2}}$, and the fact that $(a+b)^2 \le 2(a^2 + b^2)$ for $a, b \in \mathbb{R}$ gives

$$\begin{aligned}
\frac{d_2}{2} \int_{\partial\Omega} \frac{1}{v} \cdot \frac{\partial |\nabla v|^2}{\partial \nu} &\le \frac{d_2}{2} \int_{\partial\Omega} \frac{2\kappa |\nabla v|^2}{v} \\
&= \kappa d_2 \|\varphi_0(v)\|^2_{L^2(\partial\Omega)} \\
&\le \kappa d_2 \left[\varepsilon \|\nabla \varphi_0(v)\|_{L^2(\Omega)} + C(\varepsilon) \|\varphi_0(v)\|_{L^2(\Omega)} \right]^2 \\
&\le \kappa d_2 \left[2\varepsilon^2 \|\nabla \varphi_0(v)\|^2_{L^2(\Omega)} + 2C(\varepsilon)^2 \|\varphi_0(v)\|^2_{L^2(\Omega)} \right] \\
&\le \kappa d_2 \left[2\varepsilon^2 \frac{5}{4} \int_\Omega \left(\frac{|D^2 v|^2}{v} + \frac{|\nabla v|^4}{v^3} \right) + 2C(\varepsilon)^2 \int_\Omega \frac{|\nabla v|^2}{v} \right] \\
&\le \frac{A_1}{4} \int_\Omega \left(\frac{|D^2 v|^2}{v} + \frac{|\nabla v|^4}{v^3} \right) + C_1 \int_\Omega \frac{|\nabla v|^2}{v} \quad \text{for all } t \in (0, T_{\max}),
\end{aligned} \tag{3.14}$$

where $C_1 > 0$ is a constant. Now the combination of (3.10)-(3.12) and (3.14) indicates

$$I_4 \le \left[\frac{A_1}{4} - \frac{d_2}{3(2+\sqrt{2})^2 + 2} \right] \int_\Omega \left(\frac{|D^2 v|^2}{v} + \frac{|\nabla v|^4}{v^3} \right) + C_1 \int_\Omega \frac{|\nabla v|^2}{v} \quad \text{for all } t \in (0, T_{\max}),$$

which gives (3.5) by recalling $A_1 = \frac{d_2}{3(2+\sqrt{2})^2 + 2}$. Therefore, the claim (3.5) is proved, and hence (3.9) is obtained.

Step 2. Cancellation of the nonlinear term $\int_\Omega (1 + 2\alpha u) \nabla u \cdot \nabla v$. We now deal with the nonlinear term $I_5 = \int_\Omega (1 + 2\alpha u) \nabla u \cdot \nabla v$ appearing in (3.9). For all $t \in (0, T_{\max})$, using (1.6) and integration by parts, we have

$$\frac{d}{dt} \int_\Omega u \ln u = -d_1 \int_\Omega \frac{|\nabla u|^2}{u} + \chi \int_\Omega \nabla u \cdot \nabla v + \int_\Omega (1 + \ln u) f(u, v), \tag{3.15}$$

$$\frac{1}{2} \frac{d}{dt} \int_\Omega u^2 = -d_1 \int_\Omega |\nabla u|^2 + \chi \int_\Omega u \nabla u \cdot \nabla v + \int_\Omega u f(u, v), \tag{3.16}$$

$$\frac{d}{dt} \int_\Omega uv = -(d_1 + d_2) \int_\Omega \nabla u \cdot \nabla v + \chi \int_\Omega u |\nabla v|^2 + \int_\Omega v f(u, v) + \int_\Omega u g(u, v). \tag{3.17}$$

Let $A_2 := \frac{2(d_1+d_2)}{\chi} + \frac{1}{2\alpha}$. Then $\chi A_2 + \chi u - 2(d_1 + d_2) = \frac{\chi}{2\alpha}(1 + 2\alpha u)$, which alongside (3.15)-(3.17) gives

$$
\frac{d}{dt} \int_\Omega u \left(A_2 \ln u + \frac{u}{2} + 2v \right) + d_1 A_2 \int_\Omega \frac{|\nabla u|^2}{u} + d_1 \int_\Omega |\nabla u|^2
$$

$$
= \frac{\chi}{2\alpha} I_5 + 2\chi \int_\Omega u|\nabla v|^2 + \underbrace{\int_\Omega u \left(f(u, v) + 2g(u, v) \right) + A_2 \int_\Omega (1 + \ln u) f(u, v) + 2 \int_\Omega v f(u, v)}_{=: I_6} \quad (3.18)
$$

for all $t \in (0, T_{\max})$. If we multiply (3.18) by $\frac{2\alpha}{\chi}$ and add the result to (3.9), then the nonlinear term I_5 can be canceled.

Step 3. A Grönwall-type inequality. Define the function

$$
y(t) := \frac{1}{2} \int_\Omega \frac{|\nabla v|^2}{v} + \frac{2\alpha}{\chi} \int_\Omega u \left(A_2 \ln u + \frac{u}{2} + 2v \right) \quad \text{for all } t \in (0, T_{\max}). \quad (3.19)
$$

Then for all $t \in (0, T_{\max})$, the combination of (3.9) and (3.18) multiplied by $\frac{2\alpha}{\chi}$ indicates that

$$
y'(t) + y(t) + \frac{A_1}{2} \int_\Omega \left(\frac{|D^2 v|^2}{v} + \frac{|\nabla v|^4}{v^3} \right) + \frac{2\alpha}{\chi} \left(d_1 A_2 \int_\Omega \frac{|\nabla u|^2}{u} + d_1 \int_\Omega |\nabla u|^2 \right)
$$

$$
\leq C_2 + \underbrace{4\alpha \int_\Omega u|\nabla v|^2 - \frac{\alpha}{2M_0} \int_\Omega u^2|\nabla v|^2}_{=: I_7} + \underbrace{\frac{2\alpha}{\chi} \left(\int_\Omega u \left(A_2 \ln u + \frac{u}{2} + 2v \right) + I_6 \right)}_{=: I_8}. \quad (3.20)
$$

We next estimate the term I_7. Indeed, Young's inequality and (2.1) yield

$$
4\alpha \int_\Omega u|\nabla v|^2 \leq \int_\Omega \left(\frac{\alpha}{4M_0} u^2 + 16M_0\alpha \right) |\nabla v|^2
$$

$$
\leq \frac{\alpha}{4M_0} \int_\Omega u^2|\nabla v|^2 + 16M_0\alpha \int_\Omega \left(\frac{A_1}{64M_0\alpha} \frac{|\nabla v|^4}{v^3} + \frac{16M_0\alpha}{A_1} v^3 \right)
$$

$$
\leq \frac{\alpha}{4M_0} \int_\Omega u^2|\nabla v|^2 + \frac{A_1}{4} \int_\Omega \frac{|\nabla v|^4}{v^3} + \frac{256M_0^5\alpha^2}{A_1} |\Omega| \quad \text{for all } t \in (0, T_{\max}),
$$

which implies

$$
I_7 \leq -\frac{\alpha}{4M_0} \int_\Omega u^2|\nabla v|^2 + \frac{A_1}{4} \int_\Omega \frac{|\nabla v|^4}{v^3} + \frac{256M_0^5\alpha^2}{A_1} |\Omega| \quad \text{for all } t \in (0, T_{\max}). \quad (3.21)
$$

It remains to estimate the term I_8. Using (1.7), (2.1), (2.3), Young's inequality and the fact that $-s \ln s \leq \frac{1}{e}$ and $\ln s < s$ for $s > 0$, we have

$$
\int_\Omega u(f(u, v) + 2g(u, v)) = \int_\Omega u \left[-(1 + \alpha u)uv - u + 2\sigma v \left(1 - \frac{v}{K} \right) \right]
$$

$$
\leq 2\sigma M_0 M_1 - \int_\Omega (1 + \alpha u) u^2 v \quad \text{for all } t \in (0, T_{\max}).
$$

For the term I_6 included in I_8, it holds that

$$
I_6 \leq 2\sigma M_0 M_1 - \int_\Omega (1 + \alpha u) u^2 v
$$

$$
+ A_2 \int_\Omega (1 + \ln u)(1 + \alpha u) uv - A_2 \int_\Omega (1 + \ln u)u + 2M_0 \int_\Omega (1 + \alpha u) uv
$$

$$
\leq 2\sigma M_0 M_1 - \int_\Omega [u - A_2(1 + \ln u) - 2M_0](1 + \alpha u)uv + \frac{A_2}{e}|\Omega| \quad \text{for all } t \in (0, T_{\max}). \quad (3.22)
$$

Moreover, for all $t \in (0, T_{\max})$, using (2.1), (2.3) and the fact that $s^2 \geq s \ln s$ for $s \geq 0$, we obtain

$$\int_\Omega u \left(A_2 \ln u + \frac{u}{2} + 2v \right) \leq \int_\Omega u \left(A_2 u + \frac{u}{2} + 2M_0 \right) \leq (A_2 + 1) \int_\Omega u^2 + 2M_0 M_1. \tag{3.23}$$

Using (2.3), the Gagliardo–Nirenberg inequality and Young's inequality, for all $t \in (0, T_{\max})$, we can find two positive constants C_3 and C_4 such that

$$\frac{2\alpha}{\chi} (A_2 + 1) \int_\Omega u^2 \leq C_3 \left(\|\nabla u\|_{L^2(\Omega)}^{\frac{1}{2}} \|u\|_{L^1(\Omega)}^{\frac{1}{2}} + \|u\|_{L^1(\Omega)} \right)^2 \leq \frac{d_1 \alpha}{2\chi} \int_\Omega |\nabla u|^2 + C_4. \tag{3.24}$$

The combination of (3.22)-(3.24) shows that

$$I_8 \leq C_5 + \frac{d_1 \alpha}{2\chi} \int_\Omega |\nabla u|^2 - \frac{2\alpha}{\chi} \int_\Omega [u - A_2(1 + \ln u) - 2M_0] (1 + \alpha u) uv \quad \text{for all } t \in (0, T_{\max}), \tag{3.25}$$

where $C_5 := C_4 + \frac{2\alpha}{\chi} \left[2(1 + \sigma)M_0 M_1 + \frac{A_2}{e} |\Omega| \right]$. Define the function

$$\varphi(s) := -(s - A_2(1 + \ln s) - 2M_0) \qquad \text{for all } s > 0.$$

Then $\varphi'(s) = \frac{A_2}{s} - 1$ and hence

$$\varphi(s) \leq \varphi(A_2) = 2M_0 + A_2 \ln A_2 \leq 2M_0 + A_2 |\ln A_2| =: C_6.$$

Therefore, by (2.1), (2.3), (3.25) and the same argument as in deriving (3.24), we know that there exists a constant $C_7 > 0$ such that

$$\begin{aligned}
I_8 &\leq C_5 + \frac{d_1 \alpha}{2\chi} \int_\Omega |\nabla u|^2 + \frac{2\alpha}{\chi} C_6 \int_\Omega (1 + \alpha u) uv \\
&\leq C_5 + \frac{d_1 \alpha}{2\chi} \int_\Omega |\nabla u|^2 + \frac{2\alpha}{\chi} C_6 \left(M_0 M_1 + \alpha M_0 \int_\Omega u^2 \right) \\
&\leq C_7 + \frac{d_1 \alpha}{\chi} \int_\Omega |\nabla u|^2 \quad \text{for all } t \in (0, T_{\max}).
\end{aligned} \tag{3.26}$$

Substituting (3.21) and (3.26) into (3.20) yields

$$y'(t) + y(t) + \frac{A_1}{4} \int_\Omega \left(\frac{|D^2 v|^2}{v} + \frac{|\nabla v|^4}{v^3} \right) + \frac{2d_1 A_2 \alpha}{\chi} \int_\Omega \frac{|\nabla u|^2}{u} + \frac{d_1 \alpha}{\chi} \int_\Omega |\nabla u|^2 + \frac{\alpha}{4M_0} \int_\Omega u^2 |\nabla v|^2$$
$$\leq C_2 + \frac{64 M_0^5 \alpha^2}{A_1} |\Omega| + C_7 \quad \text{for all } t \in (0, T_{\max}). \tag{3.27}$$

Finally, an application of Grönwall's inequality along with the facts $u, v \geq 0$ and $u \ln u \geq -\frac{1}{e}$ yields (3.1). Furthermore, the integration of (3.27) with respect to t over $[t, t + \tau]$ gives (3.2). $\qquad \square$

3.2 The uniform-in-time estimate of $\|u(\cdot, t)\|_{L^p(\Omega)}$ for $p \geq 2$

Lemma 3.2. *Suppose that the assumptions in Theorem 1.1 hold with $n = 2$, and (u, v) is the solution of the system (1.6). Then for any $p \geq 2$, there exists a constant $C(p) > 0$ independent of t such that*

$$\|u(\cdot, t)\|_{L^p(\Omega)} \leq C(p) \quad \text{for all } t \in (0, T_{\max}). \tag{3.28}$$

Proof. Using the first equation of (1.6) and integration by parts, for all $t \in (0, T_{\max})$, we obtain

$$\begin{aligned}
\frac{1}{p} \frac{d}{dt} \int_\Omega u^p &= \int_\Omega u^{p-1} \left(d_1 \Delta u - \chi \nabla \cdot (u \nabla v) + f(u, v) \right) \\
&= -d_1(p - 1) \int_\Omega u^{p-2} |\nabla u|^2 + \chi(p - 1) \int_\Omega u^{p-1} \nabla u \cdot \nabla v + \int_\Omega u^{p-1} f(u, v). \tag{3.29}
\end{aligned}$$

For all $t \in (0, T_{\max})$, it follows from Young's inequality that

$$\chi(p-1) \int_\Omega u^{p-1} \nabla u \cdot \nabla v \leq \frac{d_1(p-1)}{4} \int_\Omega u^{p-2} |\nabla u|^2 + \frac{\chi^2(p-1)}{d_1} \int_\Omega u^p |\nabla v|^2$$

$$= \frac{d_1(p-1)}{p^2} \|\nabla u^{\frac{p}{2}}\|_{L^2(\Omega)}^2 + \frac{\chi^2(p-1)}{d_1} \int_\Omega u^p |\nabla v|^2. \tag{3.30}$$

For the last term in the right-hand side of the above inequality, we use Hölder's inequality $\|u^p |\nabla v|^2\|_{L^1(\Omega)} \leq \|u^p\|_{L^2(\Omega)} \||\nabla v|^2\|_{L^2(\Omega)}$, the Gagliardo–Nirenberg inequality and Young's inequality to find a constant $C_1 > 0$ such that

$$\frac{\chi^2(p-1)}{d_1} \int_\Omega u^p |\nabla v|^2 \leq \frac{\chi^2(p-1)}{d_1} \|u^{\frac{p}{2}}\|_{L^4(\Omega)}^2 \|\nabla v\|_{L^4(\Omega)}^2$$

$$\leq \frac{\chi^2(p-1)}{d_1} C_1 \left(\|\nabla u^{\frac{p}{2}}\|_{L^2(\Omega)} \|u^{\frac{p}{2}}\|_{L^2(\Omega)} + \|u^{\frac{p}{2}}\|_{L^2(\Omega)}^2 \right) \|\nabla v\|_{L^4(\Omega)}^2$$

$$\leq \frac{d_1(p-1)}{p^2} \|\nabla u^{\frac{p}{2}}\|_{L^2(\Omega)}^2 + \frac{p^2}{4d_1(p-1)} \left(\frac{\chi^2(p-1)}{d_1} C_1 \|u^{\frac{p}{2}}\|_{L^2(\Omega)} \|\nabla v\|_{L^4(\Omega)}^2 \right)^2$$

$$+ \frac{\chi^2(p-1)}{d_1} C_1 \|u\|_{L^p(\Omega)}^p \|\nabla v\|_{L^4(\Omega)}^2$$

$$\leq \frac{d_1(p-1)}{p^2} \|\nabla u^{\frac{p}{2}}\|_{L^2(\Omega)}^2 + \frac{p^2(p-1)\chi^4}{4d_1^3} C_1^2 \|u\|_{L^p(\Omega)}^p \|\nabla v\|_{L^4(\Omega)}^4$$

$$+ \frac{\chi^2(p-1)}{d_1} C_1 \|u\|_{L^p(\Omega)}^p \left(\|\nabla v\|_{L^4(\Omega)}^4 + 1 \right)$$

$$= \frac{d_1(p-1)}{p^2} \|\nabla u^{\frac{p}{2}}\|_{L^2(\Omega)}^2 + C_2 \|u\|_{L^p(\Omega)}^p \|\nabla v\|_{L^4(\Omega)}^4 + C_3 \int_\Omega \left(u^{p+1} + 1 \right) \tag{3.31}$$

for all $t \in (0, T_{\max})$, where

$$C_2 := \frac{p^2(p-1)\chi^4}{4d_1^3} C_1^2 + \frac{\chi^2(p-1)}{d_1} C_1 \quad \text{and} \quad C_3 := \frac{\chi^2(p-1)}{d_1} C_1.$$

For the last term in the right-hand side of (3.29), we have from (1.7), (3.1) and Young's inequality that

$$\int_\Omega u^{p-1} f(u, v) \leq \int_\Omega u^{p-1} (1 + \alpha u) \, uv \leq M_0 \int_\Omega \left(u^p + \alpha u^{p+1} \right) \leq M_0 \left(|\Omega| + (\alpha + 1) \int_\Omega u^{p+1} \right)$$

for all $t \in (0, T_{\max})$. Let $\phi(t) := \frac{1}{p} \|u(\cdot, t)\|_{L^p(\Omega)}^p$ for all $t \in (0, T_{\max})$. Then Hölder's inequality implies

$$\phi(t)^{\frac{p+1}{p}} = \left(\frac{1}{p} \right)^{\frac{p+1}{p}} \|u\|_{L^p(\Omega)}^{p+1} \leq \left(\frac{1}{p} \right)^{\frac{p+1}{p}} |\Omega|^{\frac{1}{p}} \|u\|_{L^{p+1}(\Omega)}^{p+1} \quad \text{for all } t \in (0, T_{\max}). \tag{3.32}$$

For all $t \in (0, T_{\max})$, the combination of (3.29)-(3.32) implies that

$$\phi'(t) + \phi(t)^{\frac{p+1}{p}} + \frac{2d_1(p-1)}{p^2} \|\nabla u^{\frac{p}{2}}\|_{L^2(\Omega)}^2 \leq C_2 \|u\|_{L^p(\Omega)}^p \|\nabla v\|_{L^4(\Omega)}^4 + C_4 \|u\|_{L^{p+1}(\Omega)}^{p+1} + C_3 + M_0 |\Omega|, \tag{3.33}$$

where $C_4 := C_3 + (\alpha + 1)M_0 + \left(\frac{1}{p}\right)^{\frac{p+1}{p}} |\Omega|^{\frac{1}{p}}$. Again applying the Gagliardo–Nirenberg inequality and Young's inequality, and using (3.1), one can find two positive constants C_5 and C_6 such that

$$
\begin{aligned}
C_4 \|u\|_{L^{p+1}(\Omega)}^{p+1} = C_4 \|u^{\frac{p}{2}}\|_{L^{\frac{2(p+1)}{p}}(\Omega)}^{\frac{2(p+1)}{p}} &\leq C_5 \left(\|\nabla u^{\frac{p}{2}}\|_{L^2(\Omega)}^{\frac{2(p+1)}{p} \cdot \frac{p-1}{p+1}} \|u^{\frac{p}{2}}\|_{L^{\frac{4}{p}}(\Omega)}^{\frac{2(p+1)}{p} \cdot \frac{2}{p+1}} + \|u^{\frac{p}{2}}\|_{L^{\frac{4}{p}}(\Omega)}^{\frac{2(p+1)}{p}} \right) \\
&\leq C_6 \left(\|\nabla u^{\frac{p}{2}}\|_{L^2(\Omega)}^{\frac{2(p-1)}{p}} + 1 \right) \\
&\leq \frac{d_1(p-1)}{p^2} \|\nabla u^{\frac{p}{2}}\|_{L^2(\Omega)}^2 + C_7 \quad \text{for all } t \in (0, T_{\max}),
\end{aligned}
\tag{3.34}
$$

where

$$
C_7 := \frac{1}{p} \left(\frac{p}{p-1} \frac{d_1(p-1)}{p^2} \right)^{-(p-1)} C_6^p + C_6 = \frac{1}{p} \left(\frac{p}{d_1} \right)^{p-1} C_6^p + C_6.
$$

Substituting (3.34) into (3.33), for all $t \in (0, T_{\max})$, we arrive at

$$
\phi'(t) + \phi(t)^{\frac{p+1}{p}} + \frac{d_1(p-1)}{p^2} \|\nabla u^{\frac{p}{2}}\|_{L^2(\Omega)}^2 \leq pC_2 \phi(t) \|\nabla v\|_{L^4(\Omega)}^4 + C_3 + M_0|\Omega| + C_7.
\tag{3.35}
$$

Let $\tau = \min\left\{1, \frac{T_{\max}}{2}\right\} \leq 1$. Then it follows from (2.1) and (3.2) that there exists a constant $C_8 > 0$ such that

$$
pC_2 \int_t^{t+\tau} \|\nabla v\|_{L^4(\Omega)}^4 = pC_2 \int_t^{t+\tau} \int_\Omega \frac{|\nabla v|^4}{v^3} v^3 \leq pC_2 M_0^3 \int_t^{t+\tau} \int_\Omega \frac{|\nabla v|^4}{v^3} \leq C_8(\tau + 1) \leq 2C_8
\tag{3.36}
$$

for all $t \in (0, T_{\max} - \tau)$.

We are now in a position to prove (3.28). We shall discuss two cases: $T_{\max} < 2$ and $T_{\max} \geq 2$. If $T_{\max} < 2$, then $\tau < 1$, and (2.4) implies

$$
\phi(t) \leq \phi(0) e^{\int_0^t pC_2 \|\nabla v(\cdot,s)\|_{L^4(\Omega)}^4 ds} + (C_3 + M_0|\Omega| + C_7) \int_0^t e^{\int_\tau^t pC_2 \|\nabla v(\cdot,s)\|_{L^4(\Omega)}^4 ds} d\tau
\tag{3.37}
$$

for all $t \in (0, T_{\max})$. By an argument similar to that used to derive (3.36), we have

$$
e^{\int_\tau^t pC_2 \|\nabla v(\cdot,s)\|_{L^4(\Omega)}^4 ds} \leq e^{\int_0^t pC_2 \|\nabla v(\cdot,s)\|_{L^4(\Omega)}^4 ds} \leq e^{\int_0^{T_{\max}} pC_2 \|\nabla v(\cdot,s)\|_{L^4(\Omega)}^4 ds} \leq C_9(T_{\max} + 1) \leq 3C_9.
$$

This alongside (3.37) gives

$$
\phi(t) \leq 3h(0)C_9 + 3(C_3 + M_0|\Omega| + C_7) \int_0^2 C_9 d\tau \leq 3h(0)C_9 + 6(C_3 + M_0|\Omega| + C_7)C_9,
$$

which proves (3.28) in the case of $T_{\max} < 2$. If $T_{\max} \geq 2$, then $\tau = 1$. By (2.5) and (2.6), we get

$$
\sup_{t \in (0,T_{\max})} \phi(t) = \sup_{t \in (0,T_{\max})} \frac{1}{p} \|u(\cdot,t)\|_{L^p(\Omega)}^p \leq \frac{1}{p} \left(\frac{2A}{1 + \frac{1}{p}} \right)^{p+1} + 2B,
\tag{3.38}
$$

where $A = (1 + 2C_8)^{\frac{p}{1+p}} e^{4C_8}$ and

$$
B = (C_3 + M_0|\Omega| + C_7)^{\frac{p}{1+p}} e^{4C_8} + 2(C_3 + M_0|\Omega| + C_7) e^{4C_8} + \frac{1}{p} \|u_0(\cdot)\|_{L^p(\Omega)}^p e^{2C_8}
$$

are independent of $T_{\max}$. Therefore, (3.38) yields (3.28) in the case of $T_{\max} \geq 2$. The proof is completed. $\qquad \square$

3.2.1 *Proof of Theorem 1.1 for* $n = 2$.

Lemma 3.2 gives $\|u\|_{L^4(\Omega)} \leq C$. Then Theorem 1.1 with $n = 2$ follows from (2.2) and Lemma 2.6 immediately. $\square$

4. Proof of Theorem 1.1 for $n \geq 3$

This section is devoted to proving Theorem 1.1 for $n \geq 3$ by the weighted L^p-estimates ($p > 1$). For M_0 given by (2.1) and $p > 1$, we define the following positive constants

$$\begin{cases} \Gamma_1 := \dfrac{d_2 p(p-1)}{p(d_1^2 + d_2^2) + 2d_1 d_2}, \quad \Gamma_2 := \dfrac{1}{2d_2}\sqrt{p\left(p + \tfrac{2d_2}{d_1}\right)}, \\ \Gamma_3 := \dfrac{2d_1 d_2 (p-1)}{p(d_1^2 + d_2^2) + 2d_1 d_2}, \quad \chi_p := \dfrac{\pi}{2\Gamma_2 M_0}. \end{cases} \tag{4.1}$$

We then construct the following function to be used later.

Lemma 4.1. *Let $p > 1$, $\Gamma_1, \Gamma_2, \Gamma_3$, χ_p be given by (4.1) and $\chi \in (0, \chi_p)$. Then for all $s \in [0, M_0]$, the function*

$$\varphi(s) := e^{\Gamma_1 \chi s}\left[\cos\left(\chi \Gamma_2 s\right)\right]^{-\Gamma_3} \tag{4.2}$$

satisfies

$$1 \leq \varphi(s) \leq \varphi(M_0) < +\infty, \tag{4.3}$$

$$0 < \chi \Gamma_1 \leq \frac{\varphi'(s)}{\varphi(s)} = \chi\left[\Gamma_1 + \Gamma_2 \Gamma_3 \tan\left(\chi \Gamma_2 s\right)\right] \leq \chi\left[\Gamma_1 + \Gamma_2 \Gamma_3 \tan\left(\chi \Gamma_2 M_0\right)\right] =: k_{\chi,p} < +\infty, \tag{4.4}$$

$$\frac{d_2}{p}\varphi''(s) - \chi\varphi'(s) - \frac{\left[\left(\chi(p-1)\varphi(s) - (d_1 + d_2)\varphi'(s)\right)\right]^2}{2d_1(p-1)\varphi(s)} = 0. \tag{4.5}$$

Proof. Clearly, (4.1) and $\chi \in (0, \chi_p)$ imply

$$0 < \chi \Gamma_2 s \leq \chi \Gamma_2 M_0 < \frac{\pi}{2} \quad \text{for all } s \in [0, M_0].$$

Hence (4.1) and (4.2) indicate that $\varphi(s)$ increases in $s \in [0, M_0]$ and (4.3) holds. By a simple calculation, we have

$$\frac{\varphi'(s)}{\varphi(s)} = \chi\left[\Gamma_1 + \Gamma_2 \Gamma_3 \tan\left(\chi \Gamma_2 s\right)\right] \quad \text{for all } s \in [0, M_0],$$

and then (4.4) is obvious. We next prove (4.5). By tedious calculations, we arrive at

$$2d_1(p-1)\varphi(s)\left(\frac{d_2}{p}\varphi''(s) - \chi\varphi'(s)\right) - \left[\left(\chi(p-1)\varphi(s) - (d_1 + d_2)\varphi'(s)\right)\right]^2$$

$$= -\frac{1}{p}\left(\frac{\varphi(s)}{\cos\left(\chi \Gamma_2 s\right)}\right)^2 \left\{B_1 \cos^2\left(\chi \Gamma_2 s\right) + \Gamma_2 \Gamma_3 \chi \sin\left(\chi \Gamma_2 s\right)\left[2B_2 \cos\left(\chi \Gamma_2 s\right) + B_3 \Gamma_2 \chi \sin\left(\chi \Gamma_2 s\right)\right]\right\}, \tag{4.6}$$

where

$$\begin{cases} B_1 := \Gamma_1^2 \chi^2 \left[p(d_1^2 + d_2^2) + 2d_1 d_2\right] - 2d_1 d_2 \Gamma_2^2 \Gamma_3(p-1)\chi^2 + (p-1)p\chi\left[(p-1)\chi - 2d_2 \Gamma_1 \chi\right], \\ B_2 := \Gamma_1 \chi\left[p(d_1^2 + d_2^2) + 2d_1 d_2\right] - d_2 p(p-1)\chi, \\ B_3 := \Gamma_3\left[p(d_1^2 + d_2^2) + 2d_1 d_2\right] - 2d_1 d_2(p-1). \end{cases}$$

Clearly, it follows from (4.1) that $B_2 = B_3 = 0$ and

$$B_1 = (p-1)\chi^2\left[p(p-1) - pd_2 \Gamma_1 - 2d_1 d_2 \Gamma_2^2 \Gamma_3\right] = \frac{d_1(p-1)^2 \chi^2 \left[d_1\left(p^2 - 4d_2^2 \Gamma_2^2\right) + 2d_2 p\right]}{p(d_1^2 + d_2^2) + 2d_1 d_2} = 0.$$

This along with (4.3), (4.6) and $p > 1$ proves (4.5). The proof is completed. □

Now we are in a position to use the above auxiliary function as a weight function to derive the uniform bound of $\|u(\cdot, t)\|_{L^p(\Omega)}$ for all $t \in (0, T_{max})$.

Lemma 4.2. *Suppose that the assumptions in Theorem 1.1 hold and (u, v) is the solution of the system (1.6). Let $p > 1$, $\Gamma_1, \Gamma_2, \Gamma_3$, χ_p be given by (4.1), $\chi \in (0, \chi_p)$ and $k_{\chi,p}$ be given by (4.4). Then there exists a constant $C(p) > 0$ independent of t such that*

$$\|u(\cdot, t)\|_{L^p(\Omega)} \le C(p) \quad \text{for all } t \in (0, T_{max}).$$

Proof. Let $\varphi(s)$ be defined by (4.2) for $s \in [0, M_0]$. Then (2.1) and (4.3) show that

$$1 \le \varphi(v(x, t)) \le \varphi(M_0) \quad \text{for all } (x, t) \in \Omega \times (0, T_{max}). \tag{4.7}$$

With integration by parts, one has

$$\frac{1}{p}\frac{d}{dt}\int_\Omega u^p\varphi(v) = \int_\Omega u^{p-1}\varphi(v)\left(d_1\Delta u - \chi\nabla\cdot(u\nabla v) + f(u,v)\right) + \frac{1}{p}\int_\Omega u^p\varphi'(v)\left(d_2\Delta v + g(u,v)\right)$$

$$= -d_1(p-1)\int_\Omega u^{p-2}\varphi(v)|\nabla u|^2 - \int_\Omega\left(\frac{d_2}{p}\varphi''(v) - \chi\varphi'(v)\right)u^p|\nabla v|^2$$

$$+ \underbrace{\int_\Omega\left[\chi(p-1)\varphi(v) - (d_1+d_2)\varphi'(v)\right]u^{p-1}\nabla u \cdot \nabla v}_{=:I_9}$$

$$+ \underbrace{\int_\Omega u^{p-1}\varphi(v)\left(f(u,v) + \frac{\varphi'(v)}{p\varphi(v)}ug(u,v)\right)}_{=:I_{10}} \quad \text{for all } t \in (0, T_{max}). \tag{4.8}$$

Using Young's inequality, for all $t \in (0, T_{max})$, we obtain

$$I_9 \le \frac{d_1(p-1)}{2}\int_\Omega u^{p-2}\varphi(v)|\nabla u|^2 + \int_\Omega\frac{\left[(\chi(p-1)\varphi(v) - (d_1+d_2)\varphi'(v))\right]^2}{2d_1(p-1)\varphi(v)}u^p|\nabla v|^2. \tag{4.9}$$

For the term I_{10}, it follows from (1.7) and (4.4) that

$$I_{10} = \int_\Omega u^{p-1}\varphi(v)\left\{(1+\alpha u)\,uv - u + \frac{\varphi'(v)}{p\varphi(v)}u\left[\sigma v\left(1 - \frac{v}{K}\right) - (1+\alpha u)\,uv\right]\right\}$$

$$\le \int_\Omega u^{p-1}\varphi(v)\left[(1+\alpha u)\,uv + \frac{\sigma k_{\chi,p}}{p}uv - \frac{\chi\Gamma_1}{p}(1+\alpha u)\,u^2v\right]$$

$$= \int_\Omega u^p\varphi(v)v\underbrace{\left[-(1+\alpha u)\left(\frac{\chi\Gamma_1}{p}u - 1\right) + \frac{\sigma k_{\chi,p}}{p}\right]}_{=:I_{11}} \quad \text{for all } t \in (0, T_{max}). \tag{4.10}$$

For the term I_{11}, (2.1) and (4.7) imply that

$$\int_{\left\{u < \frac{p}{\chi\Gamma_1}\right\}} I_{11} \le |\Omega|\left(\frac{p}{\chi\Gamma_1}\right)^p\varphi(M_0)M_0\left[\left(1 + \alpha\frac{p}{\chi\Gamma_1}\right) + \frac{\sigma k_{\chi,p}}{p}\right] =: C_1$$

and

$$\int_{\left\{u \ge \frac{p}{\chi\Gamma_1}\right\}} I_{11} \le \frac{\sigma k_{\chi,p}M_0}{p}\int_{\left\{u \ge \frac{p}{\chi\Gamma_1}\right\}} u^p\varphi(v) \le \frac{\sigma k_{\chi,p}M_0}{p}\int_\Omega u^p\varphi(v),$$

which along with (4.10) indicates that

$$I_{10} \le C_1 + \frac{\sigma k_{\chi,p}M_0}{p}\int_\Omega u^p\varphi(v) \quad \text{for all } t \in (0, T_{max}). \tag{4.11}$$

The combination of (4.5), (4.8), (4.9) and (4.11) yields

$$\frac{1}{p}\frac{d}{dt}\int_\Omega u^p\varphi(v) + \frac{1}{p}\int_\Omega u^p\varphi(v) + \frac{d_1(p-1)}{2}\int_\Omega u^{p-2}|\nabla u|^2\varphi(v) \le C_1 + C_2\int_\Omega u^p\varphi(v) \tag{4.12}$$

for all $t \in (0, T_{\max})$, where $C_2 := \frac{1+\sigma k_{\chi,p} M_0}{p}$. For the last term in the right-hand side of the above inequality, it follows from (4.7) and the Gagliardo–Nirenberg inequality that there exists a constant $C_{GN} > 0$ such that

$$C_2 \int_\Omega u^p \varphi(v) \leq C_2 \varphi(M_0) \|u^{\frac{p}{2}}\|^2_{L^2(\Omega)} \leq C_2 \varphi(M_0) C_{GN} \left(\|\nabla u^{\frac{p}{2}}\|^{2\theta}_{L^2(\Omega)} \|u^{\frac{p}{2}}\|^{2(1-\theta)}_{L^{\frac{2}{p}}(\Omega)} + \|u^{\frac{p}{2}}\|^2_{L^{\frac{2}{p}}(\Omega)} \right), \quad (4.13)$$

where

$$\theta = \frac{\frac{p}{2} - \frac{1}{2}}{\frac{p}{2} - \frac{1}{2} + \frac{1}{n}} \in (0, 1).$$

Since $0 < 2\theta < 2$, by Young's inequality, (2.3) and (4.7), we obtain from (4.13) that

$$\begin{aligned}
C_2 \int_\Omega u^p \varphi(v) &\leq C_2 \varphi(M_0) C_{GN} (M_1 + 1)^p \left(\|\nabla u^{\frac{p}{2}}\|^{2\theta}_{L^2(\Omega)} + 1 \right) \\
&\leq C_2 \varphi(M_0) C_{GN} (M_1 + 1)^p \left(\varepsilon_1 \|\nabla u^{\frac{p}{2}}\|^2_{L^2(\Omega)} + \varepsilon_1^{-\frac{\theta}{1-\theta}} + 1 \right) \\
&\leq \frac{d_1(p-1)}{p^2} \int_\Omega |\nabla u^{\frac{p}{2}}|^2 \varphi(v) + C_3 \\
&= \frac{d_1(p-1)}{4} \int_\Omega u^{p-2} |\nabla u|^2 \varphi(v) + C_3,
\end{aligned} \quad (4.14)$$

where

$$\varepsilon_1 := \frac{d_1(p-1)}{p^2 C_2 \varphi(M_0) C_{GN} (M_1 + 1)^p} \quad \text{and} \quad C_3 := C_2 \varphi(M_0) C_{GN} (M_1 + 1)^p \left(\varepsilon_1^{-\frac{\theta}{1-\theta}} + 1 \right).$$

Substituting (4.14) into (4.12), one has

$$\frac{1}{p} \frac{d}{dt} \int_\Omega u^p \varphi(v) + \frac{1}{p} \int_\Omega u^p \varphi(v) + \frac{d_1(p-1)}{4} \int_\Omega u^{p-2} |\nabla u|^2 \varphi(v) \leq C_1 + C_3.$$

Solving the above inequality, using (4.7), $u_0(x) \in W^{1,q}(\Omega)$ (recall $q > n$) and the Sobolev embedding $W^{1,q}(\Omega) \hookrightarrow L^p(\Omega)$, we can find two positive constants C_4 and C_5 satisfying

$$\|u(\cdot, t)\|^p_{L^p(\Omega)} \leq \int_\Omega u^p \varphi(v) \leq \max\left\{ \varphi(M_0) \|u_0\|^p_{L^p(\Omega)}, p(C_1 + C_3) \right\} \leq C_4 \left(\|u_0\|^p_{W^{1,q}(\Omega)} + 1 \right) \leq C_5$$

for all $t \in (0, T_{\max})$. This completes the proof. $\square$

4.2.1 *Proof of Theorem 1.1 for $n \geq 3$.*

By taking $p = 2n$ in (2.7) with Lemma 4.2, the result of Theorem 1.1 for $n \geq 3$ follows from Lemma 2.6 and (2.2). $\square$

5. Linear stability analysis and spatiotemporal patterns

Spatiotemporal patterns are important to understand the population distribution of biological systems. Predator–prey systems with prey-taxis can produce spatial patterns, as observed in experiments [26]. For the corresponding temporal predator–prey system of (1.1) with (1.2), hunting cooperation (1.4) can induce the Hopf bifurcations [49, 52, 60]. By incorporating diffusions for both predator and prey species, the system has Turing instability only if there is hunting cooperation and the prey species spreads faster than the predator species ($d_2 > d_1$). Moreover, the prey-taxis system (1.5) has no Turing patterns without hunting cooperation (i.e., $\alpha = 0$) [23]. We expect that prey-taxis will stabilize the system (1.5), similar to that observed in [37] and [62]. This section is devoted to investigating the effects of the interaction of prey-taxis and hunting cooperation (1.4) on the spatiotemporal distribution of population dynamics

described by (1.6). We conduct linear stability analysis and perform numerical simulations to illustrate possible spatiotemporal patterns.

Without spatial structures, (1.6) becomes the following ordinary differential system

$$\begin{cases} u_t = (1 + \alpha u)\, uv - u, \\ v_t = \sigma v \left(1 - \frac{v}{K}\right) - (1 + \alpha u)\, uv, \end{cases} \tag{5.1}$$

which has a trivial equilibrium $E_0 = (0, 0)$, a prey-only equilibrium $E_1 = (0, K)$, and possible positive equilibria $E_* = (u_*, v_*)$ solving

$$v_* = \frac{1}{1 + \alpha u_*} < 1 \quad \text{and} \quad (1 + \alpha u_*)u_* = \sigma \left(1 - \frac{v_*}{K}\right), \tag{5.2}$$

where u_* is the positive root of the equation

$$\alpha^2 u^3 + 2K\alpha u^2 + K(1 - \alpha\sigma)u + \sigma(1 - K) = 0.$$

The number of positive equilibria and the linear stability of equilibria of the system (5.1) are well studied in [49, 60]. We reorganize these results below. Define the positive constant

$$K_* = \frac{27\alpha\sigma}{2 + 9\alpha\sigma + 2(1 + 3\alpha\sigma)\sqrt{1 + 3\alpha\sigma}} \in (0, 1], \tag{5.3}$$

and the sets

$$\begin{cases} S_0 = (0, 1] \times (0, 1] \cup (1, \infty) \times (0, K_*), \\ S_1 = (0, \infty) \times (1, \infty) \cup (1, \infty) \times \{1\}, \\ S_2 = (1, \infty) \times (K_*, 1). \end{cases}$$

Then the number of positive equilibria of the system (5.1), denoted by N_0, is

$$N_0 = i \quad \text{if} \quad (\alpha\sigma, K) \in S_i, \quad i = 0, 1, 2.$$

To be precise, if $(\alpha\sigma, K) \in S_2$, then we denote the two positive equilibria by

$$(u_{1*}, v_{1*}) \text{ and } (u_{2*}, v_{2*}) \text{ with } 0 < v_{1*} < v_{2*} < 1.$$

It is easy to show that $E_0 = (0, 0)$ is a saddle, $E_1 = (0, K)$ is linearly stable for $0 < K < 1$ and linearly unstable for $K > 1$ (see also [49, Theorem 2.1]). The following results on the linear stability of positive equilibria hold.

Lemma 5.1 ([49, Theorem 2.2]). *Let K_* be given by (5.3) and*

$$\widetilde{K}_* = \frac{1 - 3\sigma + \sqrt{\sigma^2 + 6\sigma + 1}}{2} < 1, \qquad \widetilde{\alpha}_* = \frac{(\widetilde{K}_* + \sigma)(\widetilde{K}_* + 3\sigma)}{\sigma\widetilde{K}_*^2},$$

$$\widetilde{\alpha}_1(K) = \frac{(K + \sigma)^2}{K^2(K + \sigma - 1)} \quad \text{if } K > 1 - \sigma.$$

(a) *If $(\alpha\sigma, K) \in S_1$, then the unique positive equilibrium (u_*, v_*) is linearly stable for $0 < \alpha < \widetilde{\alpha}_1(K)$ and linearly unstable for $\alpha > \widetilde{\alpha}_1(K)$, and the Hopf bifurcation arise from (u_*, v_*) at $\alpha = \widetilde{\alpha}_1(K)$.*

(b) *If $(\alpha\sigma, K) \in S_2$, then (u_{2*}, v_{2*}) is linearly unstable, and for (u_{1*}, v_{1*}), we have the following results:*

   (i) *when $\sigma \geq \frac{3}{2}$, (v_{1*}, u_{1*}) is linearly stable for $\alpha < \widetilde{\alpha}_1(K)$ and linearly unstable for $\alpha > \widetilde{\alpha}_1(K)$, and the Hopf bifurcation arise from (u_*, v_*) at $\alpha = \widetilde{\alpha}_1(K)$;*

   (ii) *when $0 < \sigma < \frac{3}{2}$ and $\widetilde{K}^* < K < 1$, (v_{1*}, u_{1*}) is linearly stable for $\alpha < \widetilde{\alpha}_1(K)$ and linearly unstable for $\alpha > \widetilde{\alpha}_1(K)$, and the Hopf bifurcation arise from (u_*, v_*) at $\alpha = \widetilde{\alpha}_1(K)$;*

   (iii) *when $0 < \sigma < \frac{3}{2}$ and $K_* < K \leq \widetilde{K}^* < 1$, (v_{1*}, u_{1*}) is linearly unstable.*

5.1 Linear stability of (1.6)

Let $\Omega \subset \mathbb{R}^n$ ($n \geq 1$) be a bounded domain with smooth boundary. We now consider the stability of the constant steady states $E_1 = (0, K)$ and $E_* = (u_*, v_*)$ in the presence of spatial structure. The linearized system of (1.6) at a constant steady state $E_s = (u_s, v_s)$ is

$$
\begin{cases}
\Phi_t = \mathcal{A}\Delta\Phi + \mathcal{J}\Phi, & x \in \Omega, t > 0, \\
(v \cdot \nabla)\Phi = 0, & x \in \partial\Omega, t > 0, \\
\Phi(x, 0) = (u_0 - u_s, v_0 - v_s)^{\mathcal{T}}, & x \in \Omega,
\end{cases}
\tag{5.4}
$$

where $\mathcal{T}$ represents the transpose,

$$
\Phi = \begin{pmatrix} u - u_s \\ v - v_s \end{pmatrix}, \quad \mathcal{A} = \begin{pmatrix} d_1 & -\chi u_s \\ 0 & d_2 \end{pmatrix},
$$

and $\mathcal{J}$ is the corresponding Jacobian matrix of (5.1)

$$
\mathcal{J} = \begin{pmatrix} 2\alpha u_s v_s + v_s - 1 & u_s(1 + \alpha u_s) \\ -v_s(1 + 2\alpha u_s) & \sigma\left(1 - \frac{2v_s}{K}\right) - u_s(1 + \alpha u_s) \end{pmatrix} =: \begin{pmatrix} J_1 & J_2 \\ J_3 & J_4 \end{pmatrix}.
\tag{5.5}
$$

By the method of separation of variables, the linear system (5.4) has solutions in the form of

$$
\Phi(x, t) = \sum_{k \geq 0} (U_k, V_k)^{\mathcal{T}} e^{\rho t} \psi_k(x),
$$

where $\psi_k(x)$ is the eigenfunction of the Neumann eigenvalue problems

$$
\begin{cases}
-\Delta\psi_k(x) = k^2 \psi_k(x), & x \in \Omega, \\
\frac{\partial\psi_k(x)}{\partial v} = 0, & x \in \partial\Omega,
\end{cases}
$$

with the wave number k, the coefficients U_k and V_k are given by $(U_k, V_k)^{\mathcal{T}} = \int_\Omega \Phi(x, 0)\psi_k(x)$, and ρ is the temporal eigenvalue satisfying

$$
\rho\psi_k(x) = -k^2 \mathcal{A}\psi_k(x) + \mathcal{J}\psi_k(x).
$$

Using the above equation and the fact that the sequence $\{\psi_k\}_{k \geq 0}$ forms an orthonormal basis of $L^2(\Omega)$, we know that the two eigenvalues of the matrix $\mathcal{M}_k := -k^2 \mathcal{A} + \mathcal{J}$ are the roots of the equation

$$
\rho^2 + P_k \rho + Q_k = 0,
\tag{5.6}
$$

where

$$
P_k := (d_1 + d_2)k^2 - \beta_1, \quad Q_k := d_1 d_2 k^4 - \beta_2 k^2 + \beta_3,
\tag{5.7}
$$

and

$$
\beta_1 := J_1 + J_4, \quad \beta_2 := d_1 J_4 + d_2 J_1 + \chi u_s J_3, \quad \beta_3 := J_1 J_4 - J_2 J_3.
\tag{5.8}
$$

The two roots of (5.6), denoted by $\rho_\pm$, are given by

$$
\rho_\pm = \frac{-P_k \pm \sqrt{\Delta_{\rho_k}}}{2}, \quad \Delta_{\rho_k} := P_k^2 - 4Q_k.
\tag{5.9}
$$

Lemma 5.2. *Let $E_s = (u_s, v_s)$ be a constant steady state of the system (1.6). Then the following stability results hold for $E_s = (u_s, v_s)$.*

(i) *E_s is linearly stable if and only if $\min_{k^2 \geq 0} \{P_k, Q_k\} > 0$, and E_s is linearly unstable if and only if $\min_{k^2 \geq 0} \{P_k, Q_k\} < 0$.*

(ii) *Turing instability arises if and only if*

$$
\beta_1 < 0, \ \beta_2 > 0, \ \beta_3 > 0 \quad and \quad \min_{k^2 > 0} Q_k < 0.
$$

Proof. The first conclusion is obvious. Moreover, Turing instability arises if $E_s = (u_s, v_s)$ is linearly stable in the ODE system (5.1), while it is unstable in the PDE system (1.6). Therefore, Turing instability occurs if and only if

$$P_0 = -\beta_1 > 0, \quad Q_0 = \beta_3 > 0 \quad \text{and} \quad \min_{k^2 > 0} \{P_k, Q_k\} < 0.$$

Given (5.7), $d_1, d_2 > 0$ and $k^2 \geq 0$, the second conclusion of Lemma 5.2 follows immediately and the proof is completed. $\qquad\square$

At $E_1 = (0, K)$, $J_1 = K - 1$, $J_2 = 0$, $J_3 = -K < 0$, $J_4 = -\sigma < 0$, which imply

$$\beta_1 = K - 1 - \sigma, \quad \beta_2 = -d_1\sigma + d_2(K - 1), \quad \beta_3 = -\sigma(K - 1).$$

This indicates $\beta_2 < 0$ if $\beta_3 > 0$. Therefore, Lemma 5.2(ii) implies that Turing instability can never arise from $E_1 = (0, K)$. We next investigate whether Turing instability can arise from the positive constant steady state $E_* = (u_*, v_*)$. Let $E_s = E_*$. Then (5.5) implies

$$\mathcal{J} = \begin{pmatrix} \alpha u_* v_* & \frac{u_*}{v_*} \\ v_* - 2 & -\frac{\sigma v_*}{K} \end{pmatrix} = \begin{pmatrix} 1 - v_* & \sigma\left(1 - \frac{v_*}{K}\right) \\ v_* - 2 & -\frac{\sigma v_*}{K} \end{pmatrix}.$$

Clearly, (5.2) implies $J_3 = v_* - 2 < -1$. Hence (5.8) implies

$$\lim_{\chi \to +\infty} \beta_2 = \lim_{\chi \to +\infty} (d_1 J_4 + d_2 J_1 + \chi u_s J_3) = -\infty.$$

This alongside Lemma 5.2(ii) indicates that Turing instability cannot arise from $E_* = (u_*, v_*)$ for sufficiently large $\chi > 0$.

5.2 Spatiotemporal patterns

In this subsection, we present a specific example to illustrate the above analysis. For definiteness, we let

$$\sigma = K = d_1 = 1, \quad d_2 > 0, \quad \alpha > 0, \quad \chi \geq 0. \tag{5.10}$$

Then the system (1.6) with (5.10) admits a unique positive constant steady state $E_* = (u_*, v_*) = \left(\frac{\sqrt{\alpha} - 1}{\alpha}, \frac{1}{\sqrt{\alpha}}\right)$ if and only if $\alpha > 1$. Hence, we assume $\alpha > 1$ below. We have

$$P_k = (d_2 + 1)k^2 - \beta_1, \quad Q_k = d_2 k^4 - \beta_2 k^2 + \beta_3, \tag{5.11}$$

where

$$\beta_1 = 1 - \frac{2}{\sqrt{\alpha}}, \quad -\beta_2 = \frac{1 - (\sqrt{\alpha} - 1)d_2}{\sqrt{\alpha}} + \frac{(2\alpha - 3\sqrt{\alpha} + 1)\chi}{\alpha^{3/2}}, \quad \beta_3 = \frac{2\left(\sqrt{\alpha} - 1\right)^2}{\alpha} > 0. \tag{5.12}$$

Therefore, steady-state bifurcations occur if

$$\beta_2 > 0, \quad \varphi_Q\left(\frac{\beta_2}{2d_2}\right) < 0 \quad \text{and} \quad Q_k < 0 \text{ for some wave number } k. \tag{5.13}$$

where

$$\varphi_Q(s) := d_2 s^2 - \beta_2 s + \beta_3, \quad s \geq 0. \tag{5.14}$$

Lemma 5.3. *Let $d_2 > 0$, $\alpha > 1$, $\chi \geq 0$, (5.12) hold, and the function $\varphi_Q(s)$ be given by (5.14). Then $\beta_2 > 0$ and $\varphi_Q\left(\frac{\beta_2}{2d_2}\right) < 0$ if and only if*

$$d_2 > d_+^*(\alpha, \chi), \tag{5.15}$$

where

$$d_+^*(\alpha, \chi) := -\frac{D_1}{2D_2} - \frac{\sqrt{D_1^2 - 4D_2 D_0}}{2D_2} > 0 \tag{5.16}$$

with

$$\begin{cases} D_2 = -\left(\sqrt{\alpha}-1\right)^2 \alpha^2 < 0, \\ D_1 = 2\alpha\left(\sqrt{\alpha}-1\right)\left[\left(2\alpha-3\sqrt{\alpha}+1\right)\chi + \alpha\left(4\sqrt{\alpha}-3\right)\right] > 0, \\ D_0 = -\left[\alpha+(2\alpha-3\sqrt{\alpha}+1)\chi\right]^2 < 0. \end{cases} \tag{5.17}$$

Moreover, it holds that

$$\frac{\partial}{\partial\alpha}d_+^*(\alpha,\chi) < 0, \quad \frac{\partial}{\partial\chi}d_+^*(\alpha,\chi) > 0, \tag{5.18}$$

and for any $\chi \geq 0$, we have

$$\lim_{\alpha\to 1^+} d_+^*(\alpha,\chi) = +\infty, \quad \lim_{\alpha\to +\infty} d_+^*(\alpha,\chi) = 8. \tag{5.19}$$

Proof. Let $d_2 > 0$, $\alpha > 1$ and $\chi \geq 0$. First, (5.12) implies that $\beta_2 > 0$ is equivalent to

$$d_2 > \frac{\alpha+(2\alpha-3\sqrt{\alpha}+1)\chi}{\alpha(\sqrt{\alpha}-1)} =: d_{\alpha,\chi}^* > 0. \tag{5.20}$$

Moreover, we have from (5.12), (5.14) and (5.17) that

$$\varphi_Q\left(\frac{\beta_2}{2d_2}\right) = \frac{\varphi_*(d_2)}{4\alpha^3 d_2}, \qquad \varphi_*(d_2) := D_2 d_2^2 + D_1 d_2 + D_0. \tag{5.21}$$

It holds that $D_1^2 - 4D_2 D_0 = 32\left(\sqrt{\alpha}-1\right)^3\left(2\sqrt{\alpha}-1\right)\alpha^3\left((\sqrt{\alpha}-1)\chi+\alpha\right) > 0$, which along with $D_2, D_0 < 0$ and $D_1 > 0$ implies that $\varphi_*(d_2)$ has two positive roots

$$d_-^*(\alpha,\chi) := -\frac{D_1}{2D_2} + \frac{\sqrt{D_1^2-4D_2D_0}}{2D_2}, \quad d_+^*(\alpha,\chi) := -\frac{D_1}{2D_2} - \frac{\sqrt{D_1^2-4D_2D_0}}{2D_2}. \tag{5.22}$$

Clearly, $0 < d_-^*(\alpha,\chi) < d_+^*(\alpha,\chi)$. We next show that

$$0 < d_-^*(\alpha,\chi) < d_{\alpha,\chi}^* < d_+^*(\alpha,\chi). \tag{5.23}$$

Indeed, (5.17) and (5.22) imply

$$\begin{aligned} d_{\alpha,\chi}^* + \frac{D_1}{2D_2} &= \frac{\alpha+(2\alpha-3\sqrt{\alpha}+1)\chi}{\alpha(\sqrt{\alpha}-1)} + \frac{2\alpha\left(\sqrt{\alpha}-1\right)\left[\left(2\alpha-3\sqrt{\alpha}+1\right)\chi+\alpha\left(4\sqrt{\alpha}-3\right)\right]}{-2\left(\sqrt{\alpha}-1\right)^2\alpha^2} \\ &= \frac{\alpha+(2\alpha-3\sqrt{\alpha}+1)\chi - \left[\left(2\alpha-3\sqrt{\alpha}+1\right)\chi+\alpha\left(4\sqrt{\alpha}-3\right)\right]}{\alpha(\sqrt{\alpha}-1)} = -4, \end{aligned}$$

hence

$$-2D_2\left(d_{\alpha,\chi}^* + \frac{D_1}{2D_2}\right) = 8D_2 < 0 < \sqrt{D_1^2-4D_2D_0}.$$

This along with (5.17) indicates $d_{\alpha,\chi}^* < d_+^*(\alpha,\chi)$. Moreover, it follows from (5.17) and (5.22) that

$$\begin{aligned} \left(D_1^2-4D_2D_0\right) - \left[2D_2\left(d_{\alpha,\chi}^* + \frac{D_1}{2D_2}\right)\right]^2 &= 32\left(\sqrt{\alpha}-1\right)^3\left(2\sqrt{\alpha}-1\right)\alpha^3\left((\sqrt{\alpha}-1)\chi+\alpha\right) - (8D_2)^2 \\ &= 32\left(\sqrt{\alpha}-1\right)^3\alpha^3\left[\left(2\alpha-3\sqrt{\alpha}+1\right)\chi+\alpha\right] \\ &> 0, \end{aligned}$$

which proves $d_-^*(\alpha,\chi) < d_{\alpha,\chi}^*$. Therefore, (5.23) holds. Then the combination of (5.20)-(5.23) proves that $\beta_2 > 0$ and $\varphi_Q\left(\frac{\beta_2}{2d_2}\right) < 0$ if and only if (5.15) holds. We next prove (5.18). Since $D_2 < 0$, we have $d_+^*(\alpha,\chi) = -\frac{D_1}{2D_2} + \frac{1}{2}\sqrt{\frac{D_1^2-4D_2D_0}{D_2^2}}$. Elementary calculations (omitted for brevity) show that

$$\frac{\partial}{\partial\alpha}\left(\frac{D_1}{D_2}\right) > 0, \quad \frac{\partial}{\partial\alpha}\left(\frac{D_1^2-4D_2D_0}{D_2^2}\right) < 0 \quad \text{and} \quad \frac{\partial}{\partial\chi}\left(\frac{D_1}{D_2}\right) < 0, \quad \frac{\partial}{\partial\chi}\left(\frac{D_1^2-4D_2D_0}{D_2^2}\right) > 0,$$

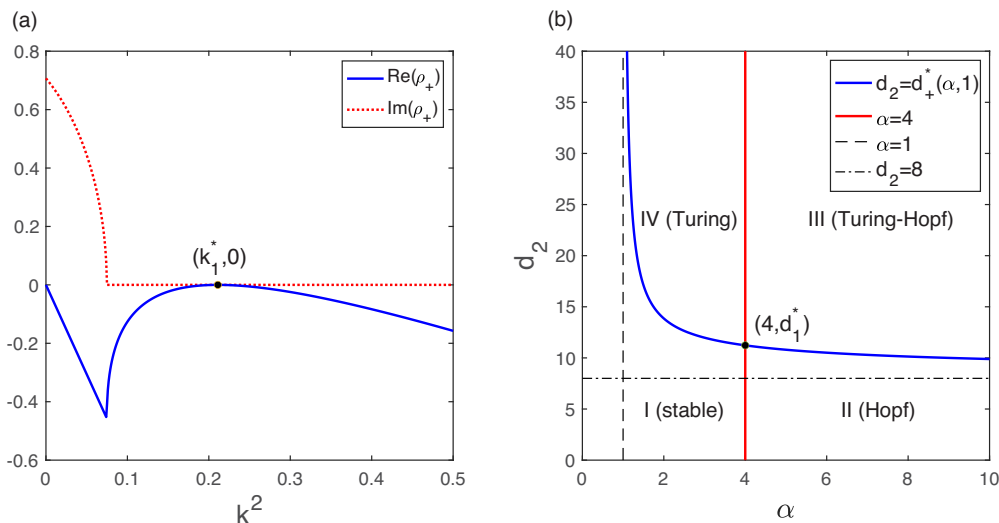**Figure 1.** *(a) Plots of $Re(\rho_+)$ and $Im(\rho_+)$ in terms of $k^2 \geq 0$ at $(\alpha, d_2) = (4, d_1^*)$, where $(d_1^*, k_1^*) \approx (11.2272, 0.2110)$ is given by (5.24) and (5.25). (b) Turing-Hopf bifurcation diagram in the α-d_2 plane, where the state-steady bifurcation curve $d_2 = d_+^*(\alpha, 1)$ given by (5.16) and the Hopf bifurcation curve $\alpha = 4$ divide the region $\{(\alpha, d_2): \alpha > 1, d_2 > 0\}$ into four parts: I (stable), II (Hopf), III (Turing–Hopf) and IV (Turing). Other parameters are given by (5.10) with $\chi = 1$.*

which along with $D_1^2 - 4D_2 D_0 > 0$ proves (5.18). Finally, we have

$$\lim_{\alpha \to +\infty} \frac{D_1}{D_2} = -8, \quad \lim_{\alpha \to +\infty} \left(\frac{D_1^2 - 4D_2 D_0}{D_2^2} \right) = 64,$$

and it is elementary to show that $\lim_{\alpha \to 1} d_+^*(\alpha, \chi) = +\infty$. Therefore (5.19) is obtained and the proof is completed. □

Clearly, (5.11) implies that Hopf bifurcations may occur if $\alpha \geq 4$ and will never occur if $\alpha \in (1, 4)$. Lemma 5.3 alongside (5.13) indicates that steady-state bifurcations may occur if $d_2 > d_+^*(\alpha, \chi)$. Moreover, steady-state bifurcations never occur if $0 < d_2 < d_+^*(\alpha, \chi)$. Indeed, the proof of Lemma 5.3 shows that $\beta_2 \leq 0$ if $0 < d_2 \leq d_{\alpha,\chi}^*$ and $\varphi_Q \left(\frac{\beta_2}{2d_2} \right) > 0$ if $d_{\alpha,\chi}^* < d_2 < d_+^*(\alpha, \chi)$, this alongside $d_2, \beta_3 > 0$ and (5.11) indicates that $Q_k > 0$ for all k if $0 < d_2 < d_+^*(\alpha, \chi)$, which means that a steady-state bifurcation is impossible. In particular, a Turing–Hopf bifurcation occurs (cf. [21, Definition 2.1 and Remark 2.2]) if $(\alpha, d_2) = (4, d_\chi^*)$, where

$$d_\chi^* := d_+^*(4, \chi) = 5 + \frac{3\chi}{4} + \sqrt{6(\chi + 4)} \geq d_0^* = 5 + 2\sqrt{6}. \tag{5.24}$$

The stability of E_* can be fully classified in the α-d_2 plane, as the following.

Lemma 5.4. *Let (5.10) hold with $\alpha > 1$ and d_χ^* be given by (5.24). Then the system (1.6) has a unique positive constant steady state $E_* = (\frac{\sqrt{\alpha}-1}{\alpha}, \frac{1}{\sqrt{\alpha}})$. Moreover, the following conclusions hold.*

(i) The ODE system (5.1) undergoes a Hopf bifurcation at $E_* = (\frac{1}{4}, \frac{1}{2})$ when $\alpha = 4$.
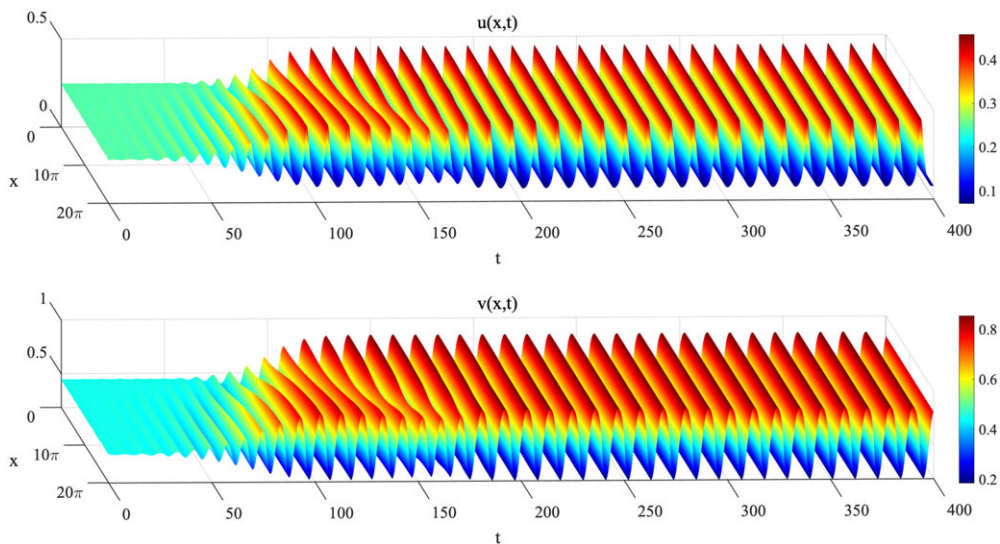
Figure 2. *Numerical simulation of spatially homogeneous time-periodic patterns generated by the system (1.6) in the interval $\Omega = (0, 20\pi)$ with (5.10), $\chi = 1$ and $\alpha = d_2 = 5$. The initial value (u_0, v_0) is set as a small random perturbation of $(u_*, v_*) = (0.0.2472, 0.4472)$.*
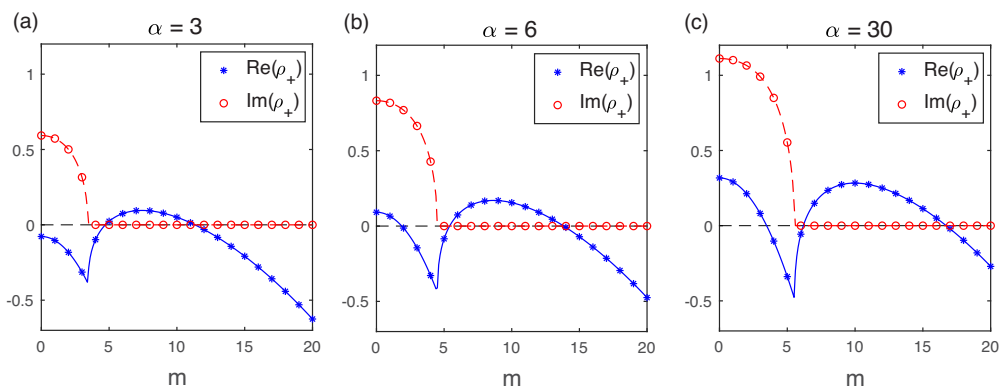

Figure 3. *Plots of $Re(\rho_+)$ and $Im(\rho_+)$ for $k = \frac{m}{20}$ with $m = 0, 1, 2, \cdots$ under the parameter setting (5.10) with $\chi = 1$, $d_2 = 20$ and different values of α: (a) $\alpha = 3$; (b) $\alpha = 6$; (c) $\alpha = 30$.*

(ii) The system (1.6) undergoes a Turing–Hopf bifurcation at $E_* = (\frac{1}{4}, \frac{1}{2})$ when $(\alpha, d_2) = (4, d_\chi^*)$. At $(\alpha, d_2) = (4, d_\chi^*)$, $\mathcal{M}_k$ has the eigenvalues

$$\begin{cases} \rho_\pm = \pm \frac{i}{\sqrt{2}}, & \text{if } k^2 = 0, \\ \rho_- = -\frac{(8+3\chi)\sqrt{6(\chi+4)}+12\chi}{4(3\chi+4)} < 0, \ \rho_+ = 0, & \text{if } k^2 = k_\chi^* := \frac{2}{\sqrt{6(\chi+4)}+4}, \\ Re(\rho_\pm) < 0, & \text{if } k^2 \neq 0, k_\chi^*. \end{cases} \tag{5.25}$$

Proof. Let $k^2 = 0$ in (5.6). Then $\rho_\pm = \pm\sqrt{Q_0} = \pm\sqrt{\beta_3} = \pm\frac{i}{\sqrt{2}}$. The first conclusion is obtained. We next prove (ii). When $(\alpha, d_2) = (4, d_\chi^*)$, we have from the proof of Lemma 5.3 that $Q_k \geq 0$, where "=" holds if and only if $k^2 = \frac{\beta_2}{2d_2} = \frac{2}{\sqrt{6(\chi+4)}+4} = k_\chi^*$. If $k^2 = k_\chi^*$, then $P_k = (d_2+1)k^2 = (d_\chi^*+1)k_\chi^* > 0$ and $Q_k = 0$, which implies $\rho_- = -P_k = -\frac{(8+3\chi)\sqrt{6(\chi+4)}+12\chi}{4(3\chi+4)} < 0$ and $\rho_+ = 0$. If $k^2 \neq 0, k_\chi^*$, then $P_k, Q_k > 0$, and hence $Re(\rho_\pm) < 0$. □
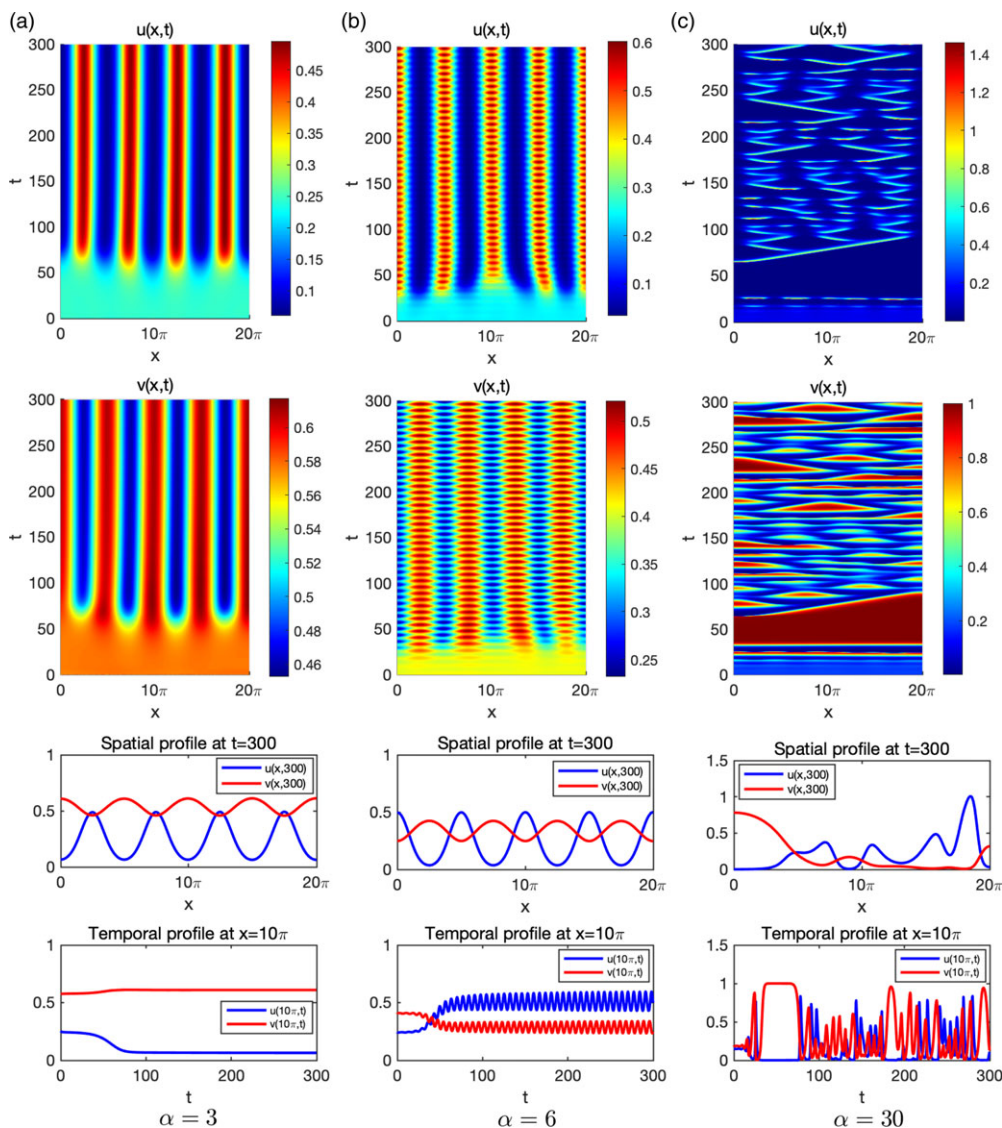
Figure 4. *Numerical simulations generated by the system (1.6) in the interval $\Omega = (0, 20\pi)$ with (5.10), $\chi = 1$, $d_2 = 20$, and different values of α shown in the columns: (a) $\alpha = 3$; (b) $\alpha = 6$; (c) $\alpha = 30$. The initial data (u_0, v_0) are set as a small random perturbation of the positive constant steady state $(u_*, v_*) = (\frac{\sqrt{\alpha}-1}{\alpha}, \frac{1}{\sqrt{\alpha}})$.*

For clarity, we shall first discuss a special case $\chi = 1$ and then turn to the general case $\chi \geq 0$.

Remark 5.1. *Fig. 1 gives an illustration for Lemma 5.4 with $\chi = 1$. Since (5.9) implies $\text{Re}(\rho_-) \leq \text{Re}(\rho_+)$, we only show the real and imaginary parts of ρ_+ in Fig. 1(a). Moreover, in the α-d_2 plane, the Hopf bifurcation curve $\alpha = 4$ and the steady state bifurcation curve $d_2 = d_+^*(\alpha, 1)$ given by Lemma 5.3 divide the region $\{(\alpha, d_2): \alpha > 1, d_2 > 0\}$ into four parts: I (stable), II (Hopf), III (Turing–Hopf) and IV (Turing).*

For numerical simulations, we let

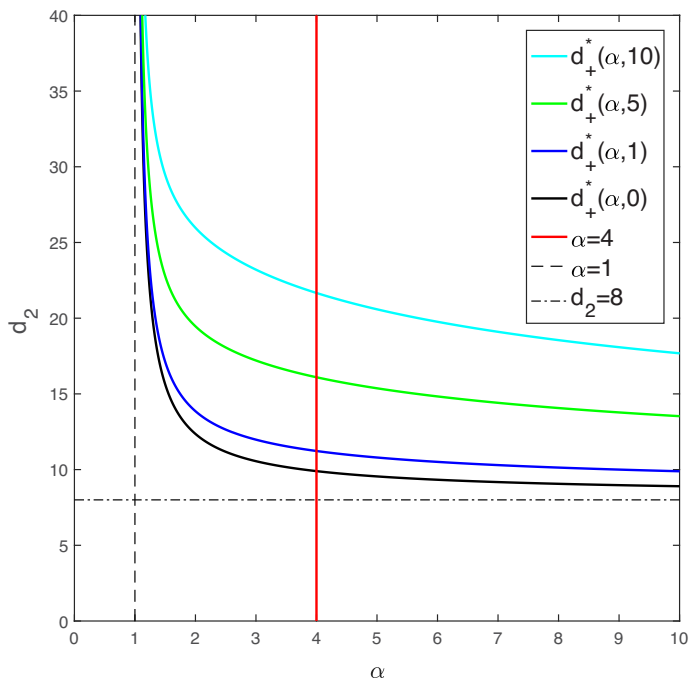$$\Omega = (0, L) \quad \text{with} \quad L = 20\pi.$$

Figure 5. *Turing–Hopf bifurcation diagram within the region $\{(\alpha, d_2): \alpha > 1, d_2 > 0\}$ in the α-d_2 plane for the system (1.6) with (5.10) and $\chi \in \{0, 1, 5, 10\}$. When (α, d_2) is above the steady state bifurcation curve $d_2 = d_+^*(\alpha, \chi)$, which given by (5.16) is higher as $\chi > 0$ is larger, the Turing instability (resp. Hopf–Turing instability) will occur if (α, d_2) is left (resp. right) to the vertical Hopf bifurcation line $\alpha = 4$.*

We begin with the subcritical case $d_2 < 8$, for which the steady-state bifurcation will never occur (see Figure 1(b) where the horizontal asymptote $d_2 = 8$ is below the steady state bifurcation curve $d_2 = d_+^*(\alpha, 1)$). Without loss of generality, we take $d_2 = 5$. Then for $\alpha \in (0, 4)$, $(\alpha, 5)$ belongs to the stable region I. In this case, (u_*, v_*) is linearly stable and no patterns will arise. For the Hopf region II, we take $\alpha = d_2 = 5$, and then the system (1.6) can generate spatially homogeneous time-periodic patterns, as shown in Figure 2. We next consider the supercritical case $d_2 > 8$. Without loss of generality, we take $d_2 = 20$ and $\alpha = 3, 6, 30$. This gives

$$(\alpha, d_2) = (3, 20) \in \text{IV}, \quad (\alpha, d_2) = (6, 20) \in \text{III}, \quad (\alpha, d_2) = (30, 20) \in \text{III}.$$

For these three values of (α, d_2), the eigenvalues ρ_+ of $\mathcal{M}_k$ with $k = \frac{m\pi}{L} = \frac{m}{20}$, $m = 0, 1, 2, \cdots$, are shown in Figure 3, and the corresponding numerical simulations are shown in Figure 4. Clearly, for $(\alpha, d_2) = (3, 20)$ in the Turing instability region IV, Figure 3(a) shows that the eigenvalues of $\mathcal{M}_k$ with $m = 0, 1, 2, 3$ are a pair of complex conjugate numbers with negative real parts, and all other eigenvalues of $\mathcal{M}_k$ with $m = 4, 5, 6, \cdots$ are real, and ρ_+ changes from negative to positive at $m = 5$. This indicates that there is a steady-state bifurcation but no Hopf bifurcation. The numerical simulations in Figure 4(a) show that non-constant stationary patterns arise, which is aligned with our analysis. For (α, d_2) in the Turing–Hopf instability region III, the system (1.6) is unstable under temporal perturbation due to Hopf bifurcation and complex eigenvalues of $\mathcal{M}_0$ have positive real parts (see Figure 3(b) and Figure 3(c) at $m = 0$), and the system (1.6) also undergoes Turing instability with real parts of an eigenvalue changing from negative to positive for some $k \neq 0$ (see Figure 3(b) with $m = 6$ and Figure 3(c) with $m = 7$ for instance). The interaction of Hopf and state-steady bifurcations will result in various complex patterns in the Turing–Hopf instability region III. For $(\alpha, d_2) = (6, 20) \in \text{III}$, spatiotemporal periodic patterns are observed, as shown in Figure 4(b). However, if we keep the diffusion rate $d_2 = 20$

and increase the strength of hunting cooperation to $\alpha = 30$, then chaotic oscillatory patterns appear as shown in Figure 4(c).

The above analysis is performed for $\chi = 1$. We next consider $\chi \geq 0$ and explain how prey-taxis stabilizes the positive constant steady state. Clearly, (5.18) and (5.19) indicate that $d_+^*(\alpha, \chi)$ strictly increases with respect to $\chi \in [0, +\infty)$, with two asymptotes: $\alpha = 1$ and $d_2 = 8$ in the α-d_2 plane. Figure 5 gives an illustration for $\chi = 0, 1, 5, 10$, where the solid blue curve $d_2 = d_+^*(\alpha, 1)$ and the red vertical line $\alpha = 4$ have been shown in Figure 1(b). The vertical coordinate of the intersection of $d_2 = d_+^*(\alpha, \chi)$ and $\alpha = 4$ is d_χ^* given by (5.24). The steady state bifurcation curve $d_+^*(\alpha, \chi)$ strictly increases in $\chi \in [0, +\infty)$ for $\alpha > 1$ (see (5.18)), while the area of stable region increases with respect to $\chi \in [0, +\infty)$, see Figure 5 for $\chi \in \{0, 1, 5, 10\}$ for instance. This indicates that prey-taxis plays a role in stabilizing the positive constant steady states.

As demonstrated above, the system (1.6) with $\chi \geq 0$ and $\alpha > 0$ may generate various spatiotemporal patterns, including spatially homogeneous time-periodic patterns, non-constant stationary patterns, spatially inhomogeneous time-periodic patterns and chaos. The former two types of patterns are also found in [6, 47, 60], where the latter two types of patterns result from the interaction of Hopf and state-steady bifurcations in the Turing–Hopf region. Moreover, we find that prey-taxis plays a stabilizing role in terms of pattern formation, which is similar to the case that the hunting cooperation functional response function adopts the Type II form [37, 62].

Competing interests. The authors declare that they have no competing interests.

References

[1] Amann, H. (1990) Dynamic theory of quasilinear parabolic equations. II. Reaction-diffusion systems. *Differ. Integral Equ* **3**(1), 13–75.

[2] Amann, H. (1993). Nonhomogeneous linear and quasilinear elliptic and parabolic boundary value problems, In *Function Spaces, Differential Operators and Nonlinear Analysis (Friedrichroda 1992)*,, Vol. 133 of Teubner-Texte Math, Teubner, Stuttgart, pp. 9–126.

[3] Arditi, R. & Ginzburg, L. R. (1989) Coupling in predator-prey dynamics: Ratio-dependence. *J. Theoret. Biol* **139**(3), 311–326.

[4] Beddington, J. R. (1975) Mutual interference between parasites or predators and its effect on searching efficiency. *J. Anim. Ecol* **44**(1), 331–340.

[5] Berec, L. (2010) Impacts of foraging facilitation among predators on predator-prey dynamics. *Bull. Math. Biol* **72**(1), 94–121.

[6] Capone, F., Maria Francesca Carfora, R. D. L. & Torcicollo, I. (2019) Turing patterns in a reaction–diffusion system modeling hunting cooperation. *Math. Compu. Simulation* **165**, 172–180.

[7] Cosner, C., DeAngelis, D. L., Ault, J. S. & Olson, D. B. (1999) Effects of spatial grouping on the functional response of predators. *Theor. Popul. Biol* **56**(1), 65–75.

[8] Creel, S. & Creel, N. M. (1995) Communal hunting and pack size in African wild dogs, lycaon pictus. *Anim. Behav* **50**(5), 1325–1339.

[9] Crowley, P. H. & Martin, E. K. (1989) Functional responses and interference within and between year classes of a dragonfly population. *J. North Amer. Benthol. Soc* **8**(3), 211–221.

[10] Donald Lee DeAngelis, R. A. G. & O'Neill, R. V. (1975) A model for tropic interaction. *Ecology* **56**(4), 881–892.

[11] Dey, S., Banerjee, M. & Ghorai, S. (2022) Bifurcation analysis and spatio-temporal patterns of a prey-predator model with hunting cooperation. *Internat. J. Bifur. Chaos Appl. Sci. Engrg* **32**(11), 19.

[12] Du, Y., Niu, B. & Wei, J. (2022) A predator-prey model with cooperative hunting in the predator and group defense in the prey. *Discrete Contin. Dyn. Syst. Ser. B* **27**(10), 5845.

[13] Grünbaum, D. (1998) Using spatially explicit models to characterize foraging performance in heterogeneous landscapes. *Amer. Nat* **151**(2), 97–113.

[14] Han, R., Dey, S. & Banerjee, M. (2023) Spatio-temporal pattern selection in a prey-predator model with hunting cooperation and Allee effect in prey. *Chaos Solitons Fractals* **171**(113441), 15.

[15] Hassell, M. P. & Varley, G. C. (1969) New inductive population model for insect parasites and its bearing on biological control. *Nature* **223**(5211), 1133–1137.

[16] Holling, C. S. (1959) The components of predation as revealed by a study of small-mammal predation of the European pine sawfly. *Can. Entomol* **91**(5), 293–320.

[17] Holling, C. S. (1959) Some characteristics of simple types of predation and parasitism. *Can. Entomol* **91**(7), 385–398.

[18] Holling, C. S. (1965) The functional response of predators to prey density and its role in mimicry and population regulation. *Mem. Entom. Soc. Can* **45**(S45), 5–60.

[19] Selwyn, L. H., Robert, H. M.jr. & Michel, P. (1987) Global existence and boundedness in reaction-diffusion systems. *SIAM J. Math. Anal* **18**(3), 744–761.

[20] Jang, S. R.-J., Zhang, W. & Larriva, V. (2018) Cooperative hunting in a predator–prey system with Allee effects in the prey. *Nat. Resour. Model* **31**(4), e12194.

[21] Jiang, W., An, Q. & Shi, J. (2020) Formulation of the normal form of Turing-Hopf bifurcation in partial functional differential equations. *J. Differ. Equ* **268**(10), 6067–6102.

[22] Jin, C. (2018) Global classical solution and stability to a coupled chemotaxis-fluid model with logistic source. *Discrete Contin. Dyn. Syst* **38**(7), 3547–3566.

[23] Jin, H.-Y. & Wang, Z.-A. (2017) Global stability of prey-taxis systems. *J. Differ. Equ* **262**(3), 1257–1290.

[24] Jin, H.-Y. & Wang, Z.-A. (2021) Global dynamics and spatio-temporal patterns of predator-prey systems with density-dependent motion. *Eur. J. Appl. Math* **32**(4), 652–682.

[25] Jin, H.-Y., Wang, Z.-A. & Wu, L. (2022) Global dynamics of a three-species spatial food chain model. *J. Differ. Equ* **333**, 144–183.

[26] Kareiva, P. & Odell, G. (1987) Swarms of predators exhibit "preytaxis" if individual predators use area-restricted search. *Amer. Natur* **130**(2), 233–270.

[27] Kruuk, H. (1972). *The Spotted Hyena: A Study of Predation and Social Behavior*, University of Chicago Press, Chicago.

[28] Liu, Y., Zhang, Z. & Li, Z. (2024) The impact of Allee effect on a Leslie-Gower predator-prey model with hunting cooperation. *Qual. Theory Dyn. Syst* **23**(2), 45.

[29] Miao, L. & He, Z. (2022) Hopf bifurcation and Turing instability in a diffusive predator-prey model with hunting cooperation. *Open Math* **20**(1), 986–997.

[30] Mizoguchi, N. & Souplet, P. (2014) Nondegeneracy of blow-up points for the parabolic Keller-Segel system. *Ann. Inst. H. Poincaré C Anal. Non Linéaire* **31**(4), 851–875.

[31] Mukherjee, N. & Banerjee, M. (2022) Hunting cooperation among slowly diffusing specialist predators can induce stationary Turing patterns. *Phys. A: Stat. Mech. Appl* **599**, 127417.

[32] Murdoch, W. W., Chesson, J. & Chesson, P. L. (1985) Biological control in theory and practice. *Amer. Nat* **125**(3), 344–366.

[33] Murie, A. (1985). *The Wolves of Mount McKinley*, University of Washington Press, Seattle.

[34] Norris, K. S. & Schilt, C. R. (1988) Cooperative societies in three-dimensional space: On the origins of aggregations, flocks, and schools, with special reference to dolphins and fish. *Ethol. Sociobiol* **9**(2–4), 149–179.

[35] Pal, S., Pal, N., Samanta, S. & Chattopadhyay, J. (2019) Effect of hunting cooperation and fear in a predator-prey model. *Ecol. Complex* **39**, 100770.

[36] Pazy, A. (1983). Semigroups of linear operators and applications to partial differential equations, Vol. 44, Applied Mathematical Sciences, Springer-Verlag, New York.

[37] Peng, Y., Yang, X. & Zhang, T. (2024) Dynamic analysis of a diffusive predator-prey model with hunting cooperation functional response and prey-taxis. *Qual. Theory Dyn. Syst* **23**(2), 22.

[38] Pierre, M. (2010) Global existence in reaction-diffusion systems with control of mass: A survey. *Milan J. Math* **78**(2), 417–455.

[39] Quittner, P. & Souplet, P. (2019). *Superlinear Parabolic Problems. Blow-up, Global Existence and Steady States*, Birkhäuser, Basel.

[40] Ryu, K. & Ko, W. (2019) Asymptotic behavior of positive solutions to a predator–prey elliptic system with strong hunting cooperation in predators. *Phys. A Stat. Mech. Appl* **531**, 121726.

[41] Ryu, K. & Ko, W. (2022) On dynamics and stationary pattern formations of a diffusive predator-prey system with hunting cooperation. *Discrete Contin. Dyn. Syst. Ser. B* **27**(11), 6679–6709.

[42] Ko, W. & Ryu, K. (2025a) A diffusive predator-prey system with hunting cooperation in predators and prey-taxis: I global existence and stability. *J. Math. Anal. Appl.* **543**(2), Paper No. 129005, 35.

[43] Ko, W. & Ryu, K. (2025b) A diffusive predator-prey system with hunting cooperation in predators and prey-taxis: II stationary pattern formation. *J. Math. Anal. Appl.* **543**(2), Paper No. 128947, 18.

[44] Sapoukhina, N., Tyutyunov, Y. & Arditi, R. (2003) The role of prey taxis in biological control: A spatial theoretical model. *Amer. Nat* **162**(1), 61–76.

[45] Scheel, D. & Packer, C. (1991) Group hunting behaviour of lions: A search for cooperation. *Anim. Behav* **41**(4), 697–709.

[46] Schmidt, P. A. & Mech, L. D. (1997) Wolf pack size and food acquisition. *Amer. Nat* **150**(4), 513–517.

[47] Singh, T., Dubey, R. & Mishra, V. N. (2020) Spatial dynamics of predator-prey system with hunting cooperation in predators and type I functional response. *AIMS Math* **5**(1), 673–684.

[48] Sk, N., Mondal, B., Sarkar, A., Santra, S. S., Baleanu, D. & Altanji, M. (2024) Chaos emergence and dissipation in a three-species food web model with intraguild predation and cooperative hunting. *AIMS Math* **9**(1), 1023–1045.

[49] Song, D., Li, C. & Song, Y. (2020) Stability and cross-diffusion-driven instability in a diffusive predator–prey system with hunting cooperation functional response. *Nonlinear Anal. Real World Appl* **54**, 103106.

[50] Song, D., Song, Y. & Li, C. (2020) Stability and Turing patterns in a predator-prey model with hunting cooperation and Allee effect in prey population. *Internat. J. Bifur. Chaos Appl. Sci. Engrg* **30**(09), 2050137.

[51] Takyi, E. M., Ohanian, C., Cathcart, M. & Kumar, N. (2024) Dynamical analysis of a predator-prey system with prey vigilance and hunting cooperation in predators. *Math. Biosci. Eng* **21**(2), 2768–2786.

[52] Alves, M. T. & Hilker, F. M. (2017) Hunting cooperation and Allee effects in predators. *J. Theoret. Biol* **419**, 13–22.

[53] Turchin, P. (2003). Complex population dynamics: A theoretical/empirical synthesis, Vol. 35, Monographs in Population Biology, Princeton University Press, Princeton, NJ.

[54] Vishwakarma, K. & Sen, M. (2022) Influence of Allee effect in prey and hunting cooperation in predator with Holling type-III functional response. *J. Appl. Math. Comput* **68**(1), 249–269.

[55] Wang, J., Shi, J. & Wei, J. (2011) Predator-prey system with strong Allee effect in prey. *J. Math. Biol* **62**(3), 291–331.

[56] Wang, X., Zanette, L. & Zou, X. (2016) Modelling the fear effect in predator-prey interactions. *J. Math. Biol* **73**(5), 1179–1204.

[57] Wang, Z. & Hillen, T. (2007) Classical solutions and pattern formation for a volume filling chemotaxis model. *Chaos* **17**(3), 037108.

[58] Wilson, E. O. (2000). *Sociobiology: The New Synthesis*, Harvard University Press.

[59] Winkler, M. (2012) Global large-data solutions in a chemotaxis-(Navier-)Stokes system modeling cellular swimming in fluid drops. *Comm. Part. Differ. Equ* **37**(2), 319–351.

[60] Wu, D. & Zhao, M. (2019) Qualitative analysis for a diffusive predator-prey model with hunting cooperative. *Phys. A: Stat. Mech. Appl* **515**, 299–309.

[61] Wu, S., Shi, J. & Wu, B. (2016) Global existence of solutions and uniform persistence of a diffusive predator-prey model with prey-taxis. *J. Differ. Equ* **260**(7), 5847–5874.

[62] Zhang, H., Fu, S. & Huang, C. (2024) Global solutions and pattern formations for a diffusive prey-predator system with hunting cooperation and prey-taxis. *Discrete Contin. Dyn. Syst. Ser. B* **29**(9), 3621–3644. doi: 10.3934/dcdsb.2024017.